

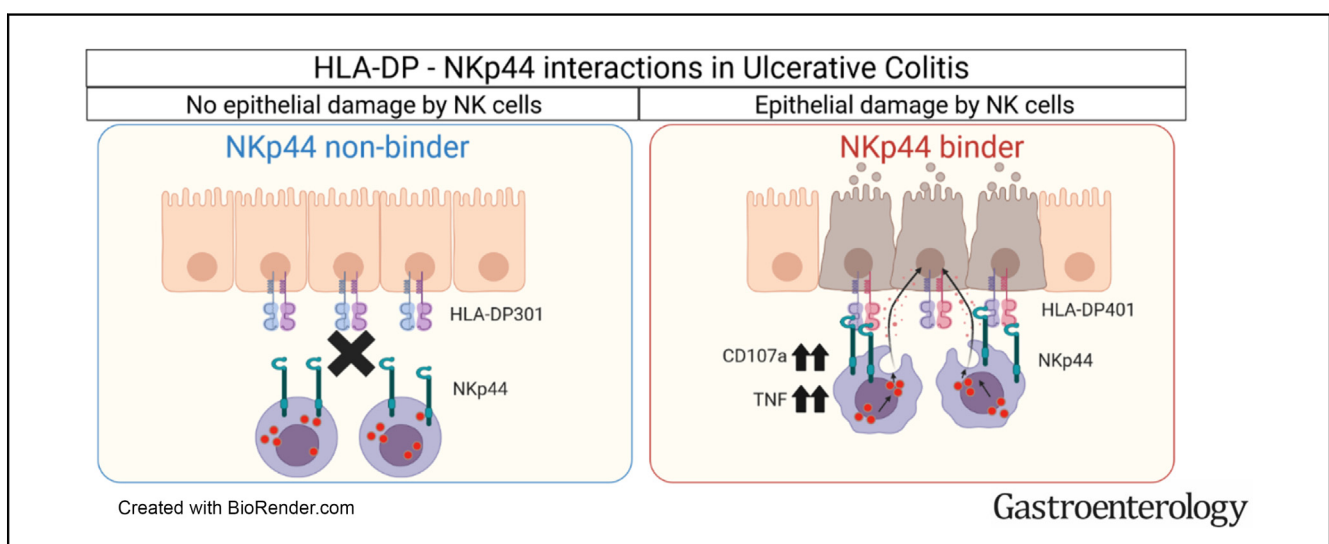
INFLAMMATORY BOWEL DISEASE

HLA-DP on Epithelial Cells Enables Tissue Damage by NKp44⁺ Natural Killer Cells in Ulcerative Colitis



Martin E. Baumdick,^{1,*} Annika Niehrs,^{1,*} Frauke Degenhardt,² Maria Schwerk,^{3,4} Ole Hinrichs,¹ Ana Jordan-Paiz,¹ Benedetta Padoan,¹ Lucy H. M. Wegner,¹ Sebastian Schloer,^{1,5} Britta F. Zecher,^{1,6} Jakob Malsy,^{1,6,7} Vinita R. Joshi,¹ Christin Illig,¹ Jennifer Schröder-Schwarz,⁸ Kimberly J. Möller,¹ Hamburg Intestinal Tissue Study Group, Maureen P. Martin,^{9,10} Yuko Yuki,^{9,10} Mikki Ozawa,¹¹ Jürgen Sauter,¹² Alexander H. Schmidt,^{12,13} Daniel Perez,¹⁴ Anastasios D. Giannou,^{14,15,16} Mary Carrington,^{9,10,17} Randall S. Davis,¹⁸ Udo Schumacher,⁸ Guido Sauter,¹⁹ Samuel Huber,^{6,15,16} Victor G. Puelles,^{3,4,20,21} Nathaniel Melling,¹⁴ Andre Franke,² on behalf of International Inflammatory Bowel Disease Genetics Consortium, **Marcus Altfeld,^{1,§}** and **Madeleine J. Bunderes^{1,3,16,22,§}**

¹Department of Virus Immunology, Leibniz Institute of Virology, Hamburg, Germany; ²Institute of Clinical Molecular Biology, Christian-Albrechts-University, Kiel, Germany; ³III. Department of Medicine, University Medical Center Hamburg-Eppendorf, Hamburg, Germany; ⁴Hamburg Center for Kidney Health, University Medical Center Hamburg-Eppendorf, Hamburg, Germany; ⁵Research Group Regulatory Mechanisms of Inflammation, Institute of Medical Biochemistry, Center for Molecular Biology of Inflammation, and Cells in Motion Interfaculty Center, University of Münster, Münster, Germany; ⁶I. Department of Medicine, University Medical Center Hamburg-Eppendorf, Hamburg, Germany; ⁷German Center for Infection Research, Hamburg-Lübeck-Borstel-Riems, Germany; ⁸Institute of Anatomy and Experimental Morphology, Center for Experimental Medicine, University Cancer Center Hamburg, University Medical Center Hamburg-Eppendorf, Hamburg, Germany; ⁹Basic Science Program, Frederick National Laboratory for Cancer Research, National Cancer Institute, Frederick, Maryland; ¹⁰Laboratory of Integrative Cancer Immunology, Center for Cancer Research, National Cancer Institute, Bethesda, Maryland; ¹¹One Lambda, Inc, Canoga Park, California; ¹²DKMS, Tübingen, Germany; ¹³DKMS Life Science Laboratory, Dresden, Germany; ¹⁴Department of General, Visceral and Thoracic Surgery, University Medical Center Hamburg-Eppendorf, Hamburg, Germany; ¹⁵Section of Molecular Immunology and Gastroenterology, I. Department of Medicine, University Medical Center Hamburg-Eppendorf, Hamburg, Germany; ¹⁶Hamburg Center for Translational Immunology, University Medical Center Hamburg-Eppendorf, Hamburg, Germany; ¹⁷Ragon Institute of MGH, MIT, and Harvard, Cambridge, Massachusetts; ¹⁸Departments of Medicine, Microbiology, and Biochemistry and Molecular Genetics, Comprehensive Cancer Center, University of Alabama at Birmingham, Birmingham, Alabama; ¹⁹Institute of Pathology, University Medical Center Hamburg-Eppendorf, Hamburg, Germany; ²⁰Department of Clinical Medicine, Aarhus University, Aarhus, Denmark; ²¹Department of Pathology, Aarhus University Hospital, Aarhus, Denmark; and ²²Section of Regenerative Medicine and Immunology, III. Department of Medicine, University Medical Center Hamburg-Eppendorf, Hamburg, Germany



BACKGROUND & AIMS: Ulcerative colitis (UC) is characterized by severe inflammation and destruction of the intestinal epithelium, and is associated with specific risk single nucleotide polymorphisms in *HLA class II*. Given the recently discovered

interactions between subsets of HLA-DP molecules and the activating natural killer (NK) cell receptor NKp44, genetic associations of UC and *HLA-DP* haplotypes and their functional implications were investigated. **METHODS:** *HLA-DP* haplotype

and UC risk association analyses were performed (UC: n = 13,927; control: n = 26,764). Expression levels of HLA-DP on intestinal epithelial cells (IECs) in individuals with and without UC were quantified. Human intestinal 3-dimensional (3D) organoid cocultures with human NK cells were used to determine functional consequences of interactions between HLA-DP and NKp44. **RESULTS:** These studies identified *HLA-DPA1*01:03-DPB1*04:01* (*HLA-DP401*) as a risk haplotype and *HLA-DPA1*01:03-DPB1*03:01* (*HLA-DP301*) as a protective haplotype for UC in European populations. HLA-DP expression was significantly higher on IECs of individuals with UC compared with controls. IECs in human intestinal 3D organoids derived from *HLA-DP401^{pos}* individuals showed significantly stronger binding of NKp44 compared with *HLA-DP301^{pos}* IECs. *HLA-DP401^{pos}* IECs in organoids triggered increased degranulation and tumor necrosis factor production by NKp44⁺ NK cells in cocultures, resulting in enhanced epithelial cell death compared with *HLA-DP301^{pos}* organoids. Blocking of HLA-DP401–NKp44 interactions (anti-NKp44) abrogated NK cell activity in cocultures. **CONCLUSIONS:** We identified an UC risk *HLA-DP* haplotype that engages NKp44 and activates NKp44⁺ NK cells, mediating damage to intestinal epithelial cells in an *HLA-DP* haplotype-dependent manner. The molecular interaction between NKp44 and HLA-DP401 in UC can be targeted by therapeutic interventions to reduce NKp44⁺ NK cell-mediated destruction of the intestinal epithelium in UC.

Keywords: Ulcerative Colitis; NK Cells; NKp44; HLA-DP; Intestinal Organoids.

Ulcerative colitis (UC) is a chronic inflammatory disease of the colon and rectum, with higher prevalence in high-income countries.¹ Current therapeutic strategies of mild to moderate UC aim to reduce inflammation with, for example, aminosalicylates or topical corticosteroids, whereas systemic corticosteroids, biologicals (ie, anti-tumor necrosis factor [TNF] or anti- $\alpha4/\beta7$) and small molecules (ie, JAK inhibitors) are used in patients with moderate to severe and steroid refractory UC cases.^{2–4} Nonetheless, even with the newest medications, frequent and severe flare-ups are observed in individuals with UC, and long-term remission is achieved in <50% of affected patients, indicating the complex mechanisms underlying UC.⁵

To maintain intestinal homeostasis, a balanced interplay between the intestinal microbiota, intestinal epithelial cells (IECs), and immune cells is required.⁶ In UC, homeostasis is disrupted and destruction of the epithelium, atrophy of crypts, and immune cell infiltration is observed.^{7,8} Although the precise etiology of UC remains unknown, multiple factors have been suggested to contribute to the pathogenesis of UC, ranging from host to environmental factors. Specifically, genes encoding HLA class I and class II have been associated with UC, as well as genes regulating epithelial cell functioning.^{9,10} Furthermore, dysregulated responses of innate immune cells, as well as CD4⁺ T cells, are observed and implicated in the pathogenesis of UC.^{11,12} Although the role of natural killer (NK) cells in UC is less investigated, NKG2A⁺ NK cells have been suggested to play a role in the

WHAT YOU NEED TO KNOW

BACKGROUND AND CONTEXT

The chronic intestinal inflammatory disease ulcerative colitis (UC) affects millions of individuals worldwide; however, the precise etiology of UC is unknown. HLA molecules have been associated with risk for UC and the recent finding that the activating NK cell receptor NKp44 binds subsets of HLA-DP molecules suggested that NK cells might contribute to intestinal inflammation.

NEW FINDINGS

A specific genotype of the HLA class II molecule HLA-DP, *HLA-DPA1*01:03-DPB1*04:01*, was identified as a UC risk haplotype. Such HLA-DP molecules expressed on intestinal epithelial cells were able to bind NKp44 and activate NKp44⁺ NK cells leading to intestinal epithelial damage.

LIMITATIONS

Our cohort consisted mainly of individuals of European ancestry and whether these interactions play a role in UC in populations of non-European ancestry needs to be further investigated.

BASIC RESEARCH RELEVANCE


Targeting the NKp44–HLA-DP interaction might constitute a promising future therapeutic approach to decrease epithelial damage by NK cells in patients with UC carrying the UC risk *HLA-DP* haplotype.

regulation of innate immune cell functions in UC.¹³ In addition, polymorphisms in killer immunoglobulin-like receptor genes, encoding for activating and inhibitory NK cell receptors that bind to HLA I molecules, have been linked to UC.^{14,15} Furthermore, innate lymphoid cells (ILCs), which share features of NK cells, have been implicated in inflammatory bowel disease (IBD).^{16,17}

Recently, our group demonstrated that the activating NK cell receptor NKp44 binds to subsets of HLA-DP molecules,¹⁸ allowing direct interactions between NK cells and HLA-DP-expressing cells. Studies by Biton et al and other groups reported that IECs can express HLA class II molecules.^{19–23} Taken together, these recent observations led us to investigate the role of specific HLA-DP/NKp44 interactions in UC. An *HLA-DP* haplotype and association analyses of individuals with UC and controls was performed and identified *HLA-DPA1*01:03-DPB1*04:01* as a risk haplotype and *HLA-DPA1*01:03-DPB1*03:01* as a protective haplotype for UC. Phenotypical characterization of colon

* Authors share co-first authorship; § Authors share co-senior authorship.

Abbreviations used in this paper: cDNA, complementary DNA; 3D, 3-dimensional; EM, expansion medium; FBS, fetal bovine serum; IBD, inflammatory bowel disease; IEC, intestinal epithelial cell; IEL, intraepithelial lymphocyte; IFN, interferon; IL, interleukin; ILC, innate lymphoid cell; NK, natural killer; TNF, tumor necrosis factor; UC, ulcerative colitis.

 Most current article

© 2023 The Author(s). Published by Elsevier Inc. on behalf of the AGA Institute. This is an open access article under the CC BY-NC-ND license (<http://creativecommons.org/licenses/by-nc-nd/4.0/>).

0016-5085

<https://doi.org/10.1053/j.gastro.2023.06.034>

samples revealed increased HLA-DP expression levels by IECs in individuals with UC. Cocultures of human intestinal 3-dimensional organoids and NK cells revealed that expression of the UC risk HLA-DP401 molecule by IECs strongly activated NKp44⁺ NK cells and induced TNF production, resulting in increased epithelial cell death in organoids, whereas the UC protective HLA-DP301 molecule did not. These findings revealed a molecular interaction between NKp44⁺ NK cells and HLA-DP401 on IECs in UC that can be targeted in therapeutic interventions to reduce NK cell-mediated epithelial tissue damage.

Materials and Methods

HLA-Haplotype Cohort Analysis

The cohort analysis included 13,927 UC cases and 26,764 controls of mostly European ancestry. *HLA-DPA1*, and *-DPB1* genotypes were imputed from quality-controlled single nucleotide polymorphism genotypes. These data, as well as genotype quality control data, have been described previously.^{9,24} To compare results from different imputation methods and imputation reference panels, we performed imputation with the Michigan Imputation Server²⁵ and using HLA genotype imputation with attribute bagging. For detailed description of both imputation methods, see the Supplementary Material.

Statistical Analysis of HLA-Haplotype Analysis

Logistic regression analysis was performed for each allele and haplotype on the case-control status for UC using the first 5 principal components derived from whole-genome single nucleotide polymorphism data.²⁴ Allele and haplotype frequencies were calculated and only alleles and haplotypes with frequencies >0.5% were retained. Alleles missing in either respective data set were assigned allele frequency <0.005. The data from both analyses were combined and corrected for multiple testing using the multiple correction method of Bonferroni-Holm. All analyses were conducted in R, version 3.6.2.

Recombinant Human Fc Construct Binding to HLA Class II-Coated Beads

Screening of HLA class II-coated beads was performed as described previously.¹⁸ In brief, recombinant human NKp44 Fc construct (2249-NK-050; R&D Systems, Minneapolis, MN), recombinant human LAG-3 Fc construct (2319_L3-050; R&D Systems), or recombinant human FcRL6 Fc construct²⁶ was incubated with a mixture of HLA class II-coated beads (LS2A01; OneLambda, Canoga Park, CA). Uncoated beads were used as negative control and IgG-coated beads as positive control. Samples were washed, incubated with a F(ab')₂ goat-anti-human IgG PE secondary antibody (10129892; Thermo Fisher, Waltham, MA) and binding of Fc constructs was quantified using Luminex xMAP technology on a Bio-Plex 200 (Bio-Rad, Hercules, CA).

Intestinal Tissue Samples

Human intestinal tissues were obtained at surgery for intestinal anastomosis reconstruction or colectomy at the University Medical Center Hamburg-Eppendorf. Collection of tissue

samples was approved by the ethics committee of the Medical Association of the Freie Hansestadt Hamburg (Ärztammer Hamburg) and donors provided written informed consent. Seventeen male and 22 female donors were included; median age was 57 years (Supplementary Table 1). They included 12 donors with UC. Control samples were obtained from individuals who underwent a tissue resection for carcinoma or reconstruction of anastomosis.

Immunohistochemistry Staining of Tissue Sections

After formalin fixation and paraffin wax embedding, sections of control and UC intestinal tissue samples were deparaffinized in Xylene and cooked at 121°C in presence of antigen retrieval solution (S1699, Dako Target Retrieval Solution; Agilent Technologies, Santa Clara, CA). Sections were incubated with HLA-DP (HPA017967; Sigma-Aldrich, St Louis, MO) or isotype control antibody (ab37415, rabbit poly IgG; Abcam, Cambridge, UK) followed by incubation with the secondary antibody (LS-C350860, goat-anti-rabbit biotinylated antibody; LSBio, Seattle, WA). Biotinylated antibody binding sites were detected with the streptavidin-alkaline phosphatase complex (AK-5000, Vectastain ABC-AP Kit; Vector Laboratories, Newark, CA), followed by visualization using liquid permanent red (ZUC001-125; Zytomed Systems, Berlin, Germany). Sections were counterstained with hemalum (1.09249.2500; Sigma-Aldrich). Images were acquired using an EVOS M5000 imaging system (Thermo Fisher).

Intestinal Epithelial Cell and Lymphocyte Isolation

IECs and intraepithelial lymphocytes (IELs) were isolated from adult intestinal tissue samples as described previously and validated to isolate the superficial epithelial layer.^{27,28} In short, the muscular layer and fat were mechanically removed from the intestinal tissue samples. IECs and IELs from intestinal tissues were obtained after incubation of the intestinal tissue samples with Iscove's modified Dulbecco's medium (10135083; Thermo Fisher Scientific) supplemented with EDTA (5 mM, V4231; Promega, Madison, WI), 1,4-dithiothreitol (6908.1; Carl-Roth GmbH+Co. KG), and 1% fetal bovine serum (FBS, FBS-11A; Capricorn, Düsseldorf, Germany). To isolate lamina propria lymphocytes, intestinal tissue, now devoid of the epithelial layer, was minced and incubated in Iscove's modified Dulbecco's medium supplemented with 1 mg/mL Collagenase D (11088882001; Sigma-Aldrich), 1% FBS, and 1000 U/mL DNaseI (07470; StemCell Technologies). The cell suspension was filtered through a 70- μ m cell strainer and lamina propria lymphocytes were obtained after a 60% standard isotonic Percoll (17-0891-62; Sigma-Aldrich) density gradient centrifugation.

For flow cytometric analyses, IECs were stained with anti-EpCAM-BV421 (#324220; Biolegend, San Diego, CA), anti-CD45-BV785 (#304048; Biolegend), anti-HLA-DP-BUV737 (#750942; BD Biosciences, San Jose, CA), anti-HLA-DQ-APC (H242-100; Leinco Technologies, St Louis, MO), anti-HLA-DR-BV711 (#307644; Biolegend), and LIVE/DEAD Fixable Near-IR Dead Cell Stain Kit (L34976; Thermo Fisher). Cells were fixed using BD Cellfix (340181; BD Biosciences) and analyzed using a BD LSR Fortessa (BD Biosciences). IELs were enriched after epithelial cell layer dissociation using density gradient centrifugation (LSM-A; Capricorn) and stained with anti-CD3-

BUV395 (#563546; BD Biosciences), anti-CD45-AF700 (#368514; Biolegend), anti-CD16-BUV737 (#612786; BD Biosciences), anti-CD56-BV785 (#362550; Biolegend), anti-NKp44-PE (#325108; Biolegend), anti-CD127-PE-Dazzle (#351336; Biolegend), anti-CD14-PE-Cy7 (#301814; Biolegend), anti-CD19-PE-Cy7 (#363012; Biolegend), anti-BDCA2-PE-Cy7 (#354214; Biolegend), anti-CD1a-PE-Cy7 (#300122; Biolegend), anti-CD123-PE-Cy7 (#306010; Biolegend), anti-CD34-PE-Cy7 (#343516; Biolegend), and LIVE/DEAD Fixable Near-IR Dead Cell Stain Kit. Fixation was performed with BD Cellfix and cells were analyzed using a BD LSR Fortessa.

RNA Isolation and Reverse Transcription Quantitative Real-Time Polymerase Chain Reaction

RNA was retrieved from cells of the intestinal epithelium using Trizol (15596018; Thermo Fisher) according to the manufacturer's instructions. RNA was treated with RNase Out (10777019; Thermo Fisher) and DNase I (AM2224; Thermo Fisher) before transcribing 1 μ g RNA into complementary DNA (cDNA) using the qScriber cDNA synthesis Kit (RTK0104, highQU; Kraichtal, Germany). cDNA templates were mixed with TNF, interferon (IFN)-gamma, glyceraldehyde 3-phosphate dehydrogenase primer pairs (Supplementary Table 2), and the QuantiFast SYBR Green PCR Kit (204057; Qiagen, Hilden, Germany). Quantitative polymerase chain reactions were performed on the Lightcycler 96 System (Roche, Basel, Switzerland). For calculating the relative gene expression, target C_T values were normalized to a reference gene (*glyceraldehyde 3-phosphate dehydrogenase*) and \log_2 transformed.

Human Intestinal Organoid Cultures

Human intestinal organoids from adult intestinal tissue samples were generated as described previously.^{28–30} In brief, isolated IECs were washed with ice-cold AD+++ (Advanced Dulbecco's modified Eagle's medium/F12 (12634-028; Thermo Fisher) containing 1% GlutaMAX (35050061; Thermo Fisher), 10 mM HEPES (15630056; Thermo Fisher), and 1% penicillin/streptomycin (P4333; Sigma-Aldrich), and resuspended in ice-cold growth factor-reduced Matrigel (356231; Corning, Corning, NY). Matrigel droplets were seeded in pre-warmed 24-well plates (662160; Greiner, Frickenhausen, Germany) and covered with expansion medium (EM; Supplementary Table 3) supplemented with 10 μ M Rho kinase inhibitor Y-27632 (72308, StemCell, Vancouver, Canada). Medium with Y-27632 was refreshed every 2–3 days until first passage. Intestinal organoids were cultured at 37°C and 5% CO₂ and passaged weekly by mechanical disruption. EM was refreshed every 2–3 days.

Human Intestinal Organoid Cytokine Stimulation

Human intestinal organoids were stimulated for 12 hours, 24 hours, 48 hours, or 72 hours with different concentrations of IFN-gamma (300-02; Pepro-Tech, Hamburg, Germany), TNF (210-TA/CF; R&D Systems), or both cytokines. Intestinal organoids were dissociated into single cells using TrypLE Express (12605028; Thermo Fisher) and used for antibody staining. Cells were stained with anti-EpCAM-BV421, anti-CD45-AF700, anti-HLA-DP-BUV737, and LIVE/DEAD Fixable

Near-IR Dead Cell Stain Kit, fixed using BD Cellfix and analyzed using a BD LSR Fortessa.

Preparation of Human Natural Killer Cells From Blood Samples

All donors provided written informed consent to obtain peripheral blood mononuclear cells and studies were approved by the Ethics Committee of the Ärztekammer Hamburg. NK cells were isolated as described previously¹⁸ and after 5–7 days stimulation with 250 U/mL interleukin (IL)-2 (200-02; Pepro-Tech) and 10 ng/mL IL-15 (200-15; Pepro-Tech) to induce NKp44 expression used for functional analyses.

Plate-Coated Natural Killer Cell and Innate Lymphoid Cell Degranulation Assay

Degranulation assays were performed as described previously.¹⁸ In brief, non-treated plates (351172; Falcon) were coated with HLA-DP401 or HLA-DP301 molecules (provided by OneLambda) or biotinylated anti-NKp44 (#325106; Biolegend). Isolated NK cells or sorted intestinal ILCs (viable singlets CD45⁺CD3⁻CD14⁻CD19⁻CD1a⁺BDCA-2⁻CD123⁻CD34⁻CD127⁺) resuspended in assay medium containing RPMI 1640 medium (12004997; Thermo Fisher) supplemented with 10% FBS or Iscove's modified Dulbecco's medium supplemented with 10% FBS were distributed on coated plates. The vesicular transport protein inhibitor brefeldin A (555029; BD Biosciences) and anti-CD107a-BV785 (#328644; Biolegend) were added, and cells were incubated for 5–8 hours. NK cells were stained with anti-CD3-BV510 (#344828; Biolegend), anti-CD56-BV605 (#318334; Biolegend), anti-CD16-FITC (#302006; Biolegend), anti-NKp44-AF647 (#325112; Biolegend), anti-TNF-PE (#502909; Biolegend), and LIVE/DEAD Fixable Near-IR Dead Cell Stain Kit. ILCs were stained with anti-CD45-AF700, anti-NKp44-AF647, anti-TNF-BUV395 (#563996; BD Biosciences), anti-IL-22-PE (#15517116; Fisher Scientific), and LIVE/DEAD Fixable Near-IR Dead Cell Stain Kit. Fixation was performed using the BD Cytofix/Cytoperm Kit (554714; BD Biosciences) and cells were analyzed using a BD LSR Fortessa.

Immunofluorescence Analyses

To de-wax formalin-fixed and paraffin wax-embedded samples, the samples were washed in Xylo 100%, followed by incubations in a descending series of ethanol. Antigen target retrieval was performed using Agilent DAKO Target Retrieval Solution (pH 9) (S236884-2; Dako) in a Braun Multiquick FS20 steamer, followed by washing in Agilent Wash Buffer Solution (K800721-2; Agilent). The staining included NCAM1/CD56 (mouse, #3576, 1:400; Cell Signaling), HLA-DPA (rb, #HPA017967, 100 μ L, 1:100; Sigma-Aldrich), AF488 donkey anti-rabbit (#A-21206, 1:200; Invitrogen), and AF647 donkey anti-mouse (#A-31571, 1:200; Invitrogen) diluted in Agilent Antibody diluent solution (K800621-2; Agilent).

Primary antibodies were incubated overnight at 4°C, followed by corresponding secondary antibodies for 1 hour. 4',6-Diamidino-2-phenylindole (D90542; Sigma-Aldrich) was added within the Agilent Antibody diluent solution to counterstain the nuclei. After washing, samples were mounted with Prolong

Gold (P36930; Thermo Fisher). Images were acquired using the LED-based widefield system THUNDER Imager 3D Live Cell and 3D Cell Culture (Leica Microsystems) in 40 \times (NA: 1.10) with Instant Computational Clearing mode.

Single-Cell Gene Expression Analysis

IELs from colon tissues were thawed and stained with anti-CD45-AF700, anti-CD3-BV510, anti-CD56-BV605, anti-CD16-FITC, anti-CD127-PE/Dazzle, and LIVE/DEAD Fixable Near-IR Dead Cell Stain Kit. Two thousand viable CD45⁺CD3⁻CD127⁻ and CD56⁺/CD16⁺ single- or double-positive NK cells were sorted from each donor, using a 5-laser FACS Aria-Fusion (BD Biosciences). Cells were captured in Single Cell Preamp IFCs, 5–10 μ m (Fluidigm) and used to generate cDNA. Further analysis included capture sites with 1 single cell. cDNA was generated according to the company protocol and gene expression was analyzed using Biomark HD 192.24 Dynamic Array IFCs for Gene Expression.

NKp44 Fc Binding to Intestinal Epithelial Cells

IFN-gamma-stimulated intestinal organoids (200 U/mL for 3–4 days) were dissociated into single cells using TrypLE Express, treated with 1 U/mL Proteinase K (19131, Qiagen) and rested in EM + Y-27632 at 37°C and 5% CO₂. Cells were washed with phosphate-buffered saline (D8537; Sigma-Aldrich) and stained with LIVE/DEAD Fixable Near-IR Dead Cell Stain Kit, NKp44-Fc (25 μ g/mL), secondary antibody F(ab) anti-human IgG-PE and anti-HLA-DP BUV737. Fixation was performed with 4% paraformaldehyde (P6148; Sigma-Aldrich) and cells were analyzed using a BD LSR Fortessa.

Coculture of Natural Killer Cells and Intestinal Epithelial Cells

In NK cell-IEC cocultures, NK cell donors were matched for HLA class I genotypes to organoid donors to reduce allogenic reactions. All donors had heterozygous alleles encoding for the epitopes C1/C2 and had at least 1 allele of *Bw4*. NK cells were isolated as described above and cultured for 6–7 days in RPMI 1640 supplemented with 10% FBS, 250 U/mL IL-2, and 10 ng/mL IL-15. Unstimulated and IFN-gamma-stimulated intestinal organoids (3 days with 200 U/mL) were dissociated into single cells with TrypLE, treated with 1 U/mL Proteinase K and counted to enumerate the number of target cells. Enriched NK cells were co-incubated with IECs at an effector to target cell ratio of 1:2 for 5 hours in RPMI 1640 with 10% FBS. In addition, anti-CD107a-BV785 antibody, brefeldin A and anti-HLA-DP (10 μ g/mL, H266; Leinco) were added. For blocking experiments, NK cells were pre-incubated in the presence of an anti-NKp44 antibody (30 μ g/mL, #325122; Biolegend) or an isotype control antibody (30 μ g/mL, #400166; Biolegend) for 30 minutes at 37°C. Cells were washed with phosphate-buffered saline, stained with anti-CD3-BV510, anti-CD16-FITC, anti-CD56-BV605, anti-NKp44-AF647, anti-TNF-PE, anti-HLA-DP-BUV737, and LIVE/DEAD Fixable Near-IR Dead Cell Stain Kit; fixed using the BD Cytotfix/Cytoperm Kit; and analyzed using a BD LSR Fortessa. The percentage of NKp44 down-regulation was calculated as: (% NKp44⁺ cells of CD56⁺ NK cells after coculture with DP⁻ IECs) – (% NKp44⁺ cells of CD56⁺ NK cells after coculture with DP⁺ IECs). The percentage of CD107a up-regulation was calculated as: (% CD107a⁺ cells of

CD56⁺ NK cells after coculture with DP⁺ IECs) – (% CD107a⁺ cells of CD56⁺ NK cells after coculture with DP⁻ IECs).

Coculture of Natural Killer Cells and Intestinal Organoids

NK cell donors were matched to organoid donors as described above, and NK cells were isolated and stimulated to induce NKp44 expression. IFN-gamma-stimulated intestinal organoids (3–4 days with 200 U/mL) were stained with 2 μ M Calcein (65-0853-78; Thermo Fisher) and organoids derived from 1 reference well were dissociated into single cells and counted to enumerate the number of target cells. Sorted viable CD3⁻, CD16⁻, CD56⁺ NK cells were co-incubated with intestinal organoids at an estimated effector to target cell ratio of 1:1 for 6 hours in RPMI 1640 with 10% FBS and anti-HLA-DP (10 μ g/mL, H266; Leinco). Cocultures were monitored using the spheroid module of the Incucyte SX5 Live Cell Imaging Analysis Instrument (Sartorius, Göttingen, Germany). The size of individual organoids was measured at 0 hours and 6 hours of co-incubation using Fiji. The normalized organoid size was calculated as follows: (organoid size at 6 hours) / (organoid size at 0 hours). To determine viability of IECs in intestinal organoid - NK cell cocultures, these were harvested after 16 hours incubation and dissociated into single cells. Cells were washed with phosphate-buffered saline, stained with anti-CD45-BUV395 (#563792; BD Biosciences), anti-EPCAM-BV421 and LIVE/DEAD Fixable Near-IR Dead Cell Stain Kit, fixed using the BD Cytotfix/Cytoperm Kit and analyzed using a BD LSR Fortessa. To determine the effect of blocking of NKp44, NK cells were pre-incubated in the presence of an anti-NKp44 antibody (30 μ g/mL, #325122; Biolegend) or an isotype control antibody (#400166; Biolegend) for 30 minutes at 37°C before adding to the intestinal organoids.

Software

BD FACS Diva (BD Biosciences) was used to acquire flow cytometric data and FlowJo (version 10.8.1; Treestar) was used to analyze flow cytometric data. GraphPad Prism, Version 9.4.0 for Windows, (www.graphpad.com) was used for graphical display and statistical analysis. ImageJ (<http://imagej.nih.gov/ij/>) was used for organoid annotation and image display. Software used for the HLA-DP haplotype and association analyses is described above.

Statistical Analysis

GraphPad Prism 9 was used to perform statistical analyses including Wilcoxon signed match rank tests, Mann-Whitney U tests, and ordinary 2-way analysis of variance and Spearman's rank correlations. HLA-DP haplotype and association analyses are described above.

Results

HLA-DP Haplotype Analyses Reveal HLA-DPA1*01:03-DPB1*04:01 as a Risk Haplotype for Ulcerative Colitis and HLA-DPA1*01:03-DPB1*03:01 and HLA-DPA1*02:01-DPB1*11:01 as Protective Haplotypes

To investigate whether individuals carrying certain HLA-DP haplotypes exhibit higher or lower risk of developing UC,

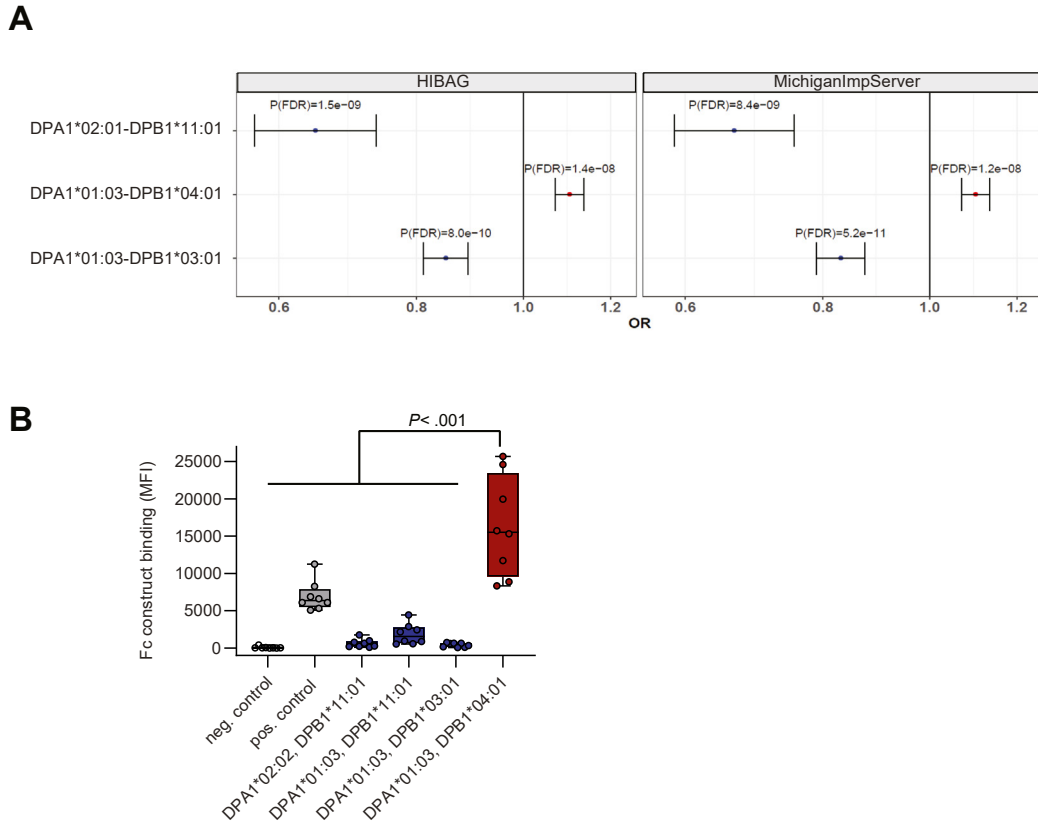


Figure 1. HLA-DP risk haplotype for UC binds to NKp44. (A) Imputation of *HLA-DPA1-DPB1* genotypes using HLA genotype imputation with attribute bagging (left) and Michigan Imputation Server (right) showing UC risk and protective *HLA-DPA1-DPB1* haplotypes with a frequency of >1% and a false discovery rate *P* (*P*[FDR]) of <.05. Odds ratios (OR) and 95% CIs are shown. (B) NKp44 Fc construct binding to beads coated with different HLA-DP molecules was determined and medians of fluorescence intensity (MFIs) of all individual experiments (*n* = 8) are depicted. Boxes indicate medians with 25% and 75% quartile ranges, and whiskers indicate minimum and maximum MFI of each HLA-DP molecule tested. HLA-DP molecules that exhibited higher median binding to the NKp44 Fc construct than to the positive control (IgG-coated beads) are marked in red and less in blue. Statistical significance was measured using Mann-Whitney U comparisons.

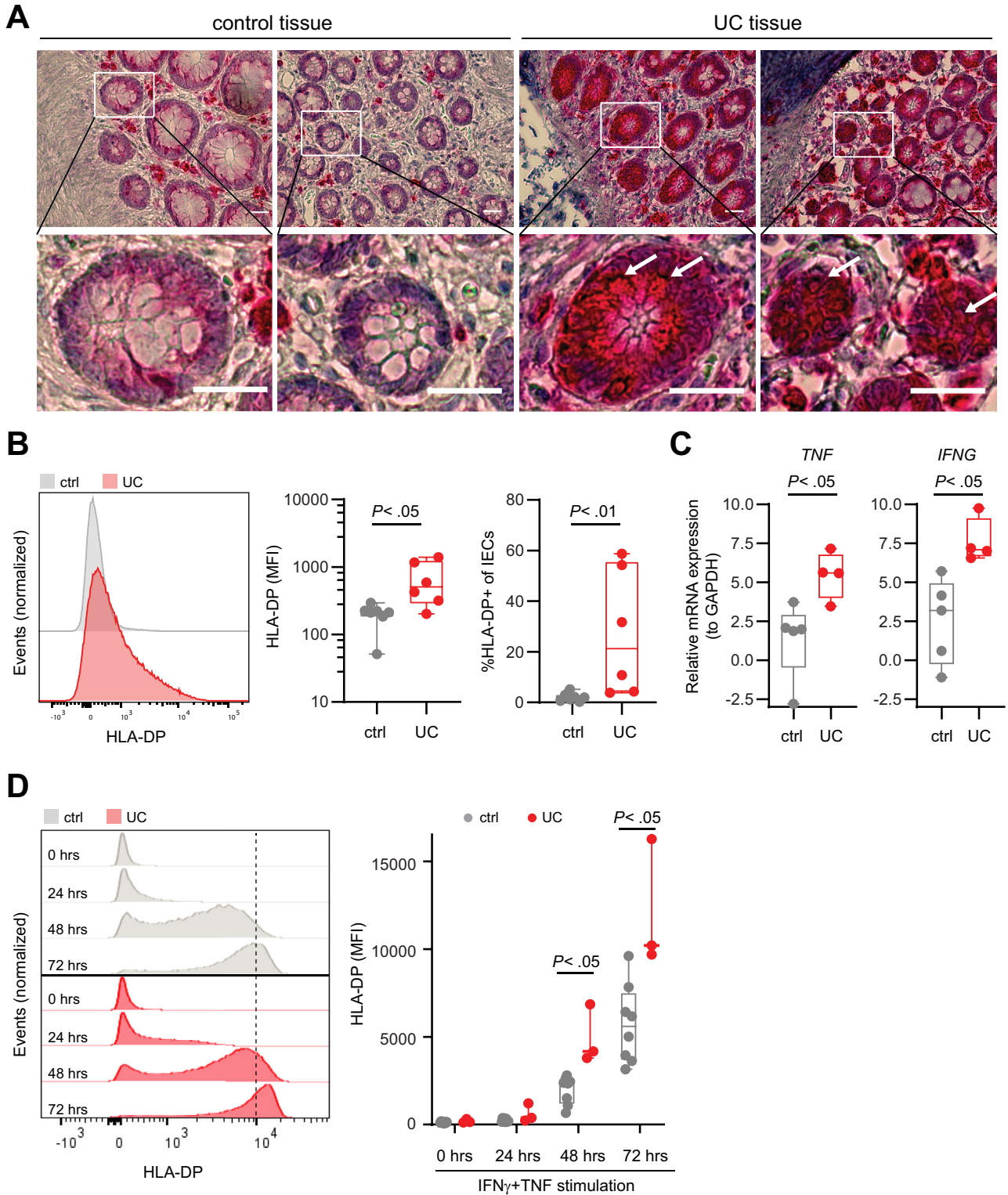
we performed an *HLA-DP* haplotype and association analyses of 13,927 individuals with UC and 26,764 control individuals of mainly European ancestry. *HLA-DPA1* and *-DPB1* genotypes were imputed from quality-controlled single nucleotide polymorphisms, and results of the 2 different imputation methods, HLA genotype imputation with attribute bagging³¹ and the Michigan Imputation Server²⁵ were compared and revealed similar outcomes. Out of a total of 21 imputed *HLA-DPA1-DPB1* haplotypes, including 3 *HLA-DPA1* alleles and 17 *HLA-DPB1* alleles, 2 protective *HLA-DPA1-DPB1* haplotypes and 1 risk *HLA-DPA1-DPB1* haplotype with allele frequencies >1% and *P* < .05 were identified for UC after correction for multiple testing (Figure 1A, Supplementary Figure 1A, and Supplementary Table 4). The haplotypes *HLA-DPA1*02:01-DPB1*11:01* and *HLA-DPA1*01:03-DPB1*03:01* were associated with a decreased risk of developing UC. In contrast, *HLA-DPA1*01:03-DPB1*04:01* was identified as a risk haplotype for UC (Figure 1A).

Building on our recent findings that subsets of HLA-DP molecules serve as ligands for the activating NK cell receptor NKp44,¹⁸ the binding of the above-identified UC-

associated *HLA-DP* haplotypes to NKp44 was assessed using an NKp44 Fc construct and Luminex technology. Due to unavailability of *HLA-DPA1*02:01-DPB1*11:01* molecules for this assay, *HLA-DPB1*11:01* molecules in combination with 2 other α -chains, *HLA-DPA1*02:02* and *-DPA1*01:03* were used. The UC protective *HLA-DPB1*11:01* molecule in combination with both HLA-DP α -chains, and the *HLA-DPA1*01:03-DPB1*03:01* (*HLA-DP301*) molecule did not bind the NKp44 Fc construct, whereas the UC risk molecule *HLA-DPA1*01:03-DPB1*04:01* (*HLA-DP401*) exhibited significantly stronger binding to the NKp44 Fc construct across multiple experiments (Figure 1B). In contrast, we did not detect binding of NKp44 Fc construct to previously identified HLA-DR or HLA-DQ UC risk and protective molecules^{9,24,32,33} (Supplementary Table 5 and Supplementary Figure 1B). NK cell receptors, LAG-3 and FcRL6, have also been described to bind to HLA class II molecules,^{26,34} however, no differential binding to previously described HLA-DR, -DQ, or -DP haplotypes associated with UC was observed (Supplementary Figure 2A and B). These results confirm the specific interactions between *HLA-DP401* and NKp44 molecules,¹⁸ and provided rational

for further analyses into a potential role for NKp44-HLA-DP interactions in UC. Because *HLA-DPA1*01:03-DPB1*04:01* (haplotype frequency: 43.29%) as a risk haplotype and *HLA-DPA1*01:03-DPB1*03:01* (haplotype

frequency: 10.01%) as a protective haplotype for UC belong to the most common haplotypes in the European population,³⁵ we focused on these 2 *HLA-DP* haplotypes in further analyses.



Intestinal Epithelial Cells of Individuals With Ulcerative Colitis Express High Levels of HLA-DP

To further determine whether HLA-DP is available for NKp44–HLA-DP interactions in UC, expression of HLA-DP molecules in colon-derived samples of individuals with UC was compared with controls. Immunohistochemical analyses showed HLA-DP⁺ cells in intestinal crypts of individuals with UC, whereas HLA-DP expression was almost absent in intestinal crypts of controls (Figure 2A; Supplementary Figure 3A). To further quantify the expression of HLA-DP on primary human IECs, flow cytometric analyses of colon-derived IECs of individuals with UC and controls were performed. Expression levels of HLA-DP on EpCAM⁺CD45⁻ IECs of individuals with UC were significantly higher compared with controls, whereas HLA-DP expression levels of CD45⁺EPCAM⁻ immune cells were lower and did not significantly differ between individuals with UC and controls (Figure 2B, Supplementary Figure 3B, C, and D). As the expression of HLA class II molecules is regulated by the transcription factor class II transactivator,³⁶ we also investigated the expression levels of other HLA class II molecules. HLA-DR expression was significantly higher on IECs of individuals with UC compared with controls (Supplementary Figure 3E), whereas HLA-DQ expression levels did not significantly differ between individuals with UC and controls (Supplementary Figure 3F). These data demonstrate a significantly higher expression of HLA-DP molecules on human IECs of individuals with UC.

Tumor Necrosis Factor and Interferon-Gamma Up-Regulate HLA-DP Expression by Intestinal Epithelial Cells

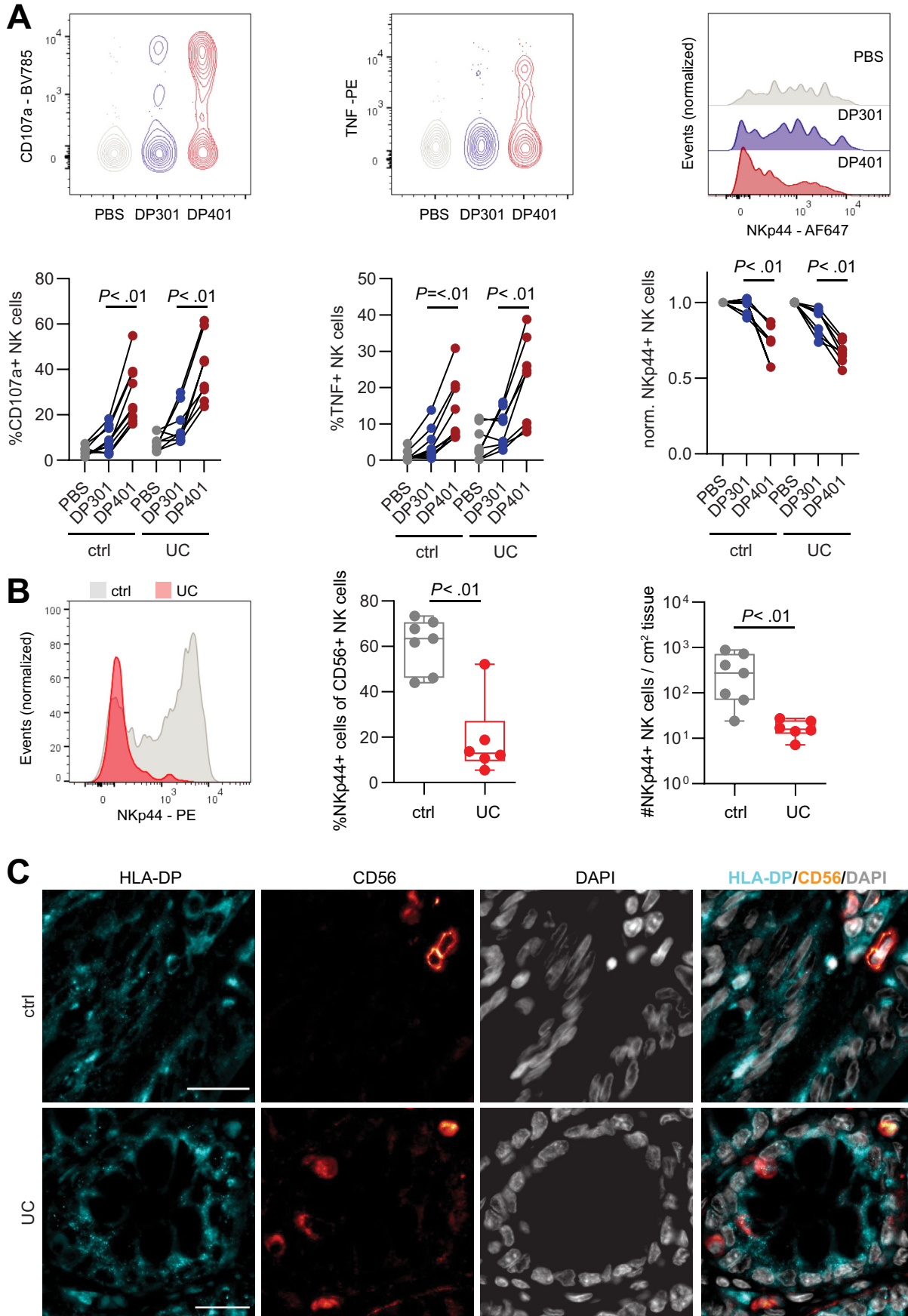
The pro-inflammatory cytokines IFN-gamma and TNF are involved in transcription factor class II transactivator-dependent up-regulation of HLA-class II molecules.^{37,38} TNF and IFNG were significantly up-regulated in the intestinal epithelium of individuals with UC compared with controls (Figure 2C). To further assess the impact of TNF and IFN-gamma on HLA-DP expression of IECs, we generated adult stem cell-derived human colon organoids from intestinal tissues of individuals with UC or controls, as described previously.^{28–30} Organoids generated from colon were stimulated with different concentrations of TNF, IFN-gamma, or a combination of both cytokines from 12 hours up to 3 days, and expression of HLA-DP molecules was

quantified over time using flow cytometric analyses. IFN-gamma stimulation induced increased expression of HLA-DP molecules on EpCAM⁺ IECs in colon organoids over time (Supplementary Figure 4A–C). This effect of IFN-gamma was further enhanced by addition of TNF (Supplementary Figure 4B), whereas stimulation with TNF alone did not induce HLA-DP protein expression on IECs in colon organoids (Supplementary Figure 4B and C). Remarkably, the up-regulation of HLA-DP molecules on dual stimulation with IFN-gamma and TNF was significantly higher on IECs in organoids generated from UC-affected colon compared with controls (Figure 2D). Previously, increased expression of HLA-DP301 compared with HLA-DP401 molecules has been described.³⁹ A trend towards increased expression of HLA-DP by HLA-DP301⁺ IECs compared with HLA-DP401⁺ IECs was observed (Supplementary Figure 4D), in line with previous studies.³⁹ Together, these results demonstrate that IFN-gamma alone and in synergy with TNF induces HLA-DP expression by IECs, including the UC risk HLA-DP401 molecule. Furthermore, IECs from UC tissues maintained an enhanced pro-inflammatory response to IFN-gamma and TNF over time in organoids.

HLA-DP401 Engagement Activates NKp44⁺ Natural Killer Cells

Binding of activating NK cell receptors to their respective ligands leads to activation, degranulation, cytokine production, and receptor internalization.⁴⁰ We next investigated whether haplotype-specific HLA-DP recognition activated NK cells from individuals with UC and controls. NKp44 expression by peripheral blood-derived NK cells was induced on culture with IL-2 and IL-15.⁴¹ Culture with HLA-DP401 molecules triggered NK cell degranulation (CD107a) and TNF production to similar levels as the positive control (anti-NKp44) and significantly higher compared with HLA-DP301 molecules for NK cells from both healthy controls and individuals with UC (Figure 3A, Supplementary Figure 5A and B). In line with NKp44-mediated activation, NKp44 expression on NK cells was significantly decreased after engagement with HLA-DP401, but not with HLA-DP301 molecules, in healthy individuals and individuals with UC (Figure 3A). These data demonstrate that binding of NKp44 to HLA-DP401, but not HLA-DP301 molecules, activates NK cells from individuals with UC and controls in a haplotype-dependent manner, and

Figure 2. High HLA-DP expression on IECs of individuals with UC. (A) Images of immunohistochemical analyses of control and UC colons. Specific HLA-DP expression is labeled in red, hemalum was used as a nuclear counterstain (blue). Lower row shows magnifications of the selected ROI (white box in images of upper row). White arrows point to HLA-DP-expressing cells. Scale bars: 250 μ m. (B) Representative histograms of HLA-DP expression in EpCAM⁺ IECs of control (ctrl) and individuals with UC measured by flow cytometry (left panel). Expression of HLA-DP (MFI) on EpCAM⁺ IECs (middle panel). Median percentages of HLA-DP⁺ cells of EpCAM⁺ IECs of controls (n = 7) and individuals with UC (n = 6) (right panel). (C) Relative messenger RNA expression of TNF and IFNG to reference gene GAPDH in the intestinal epithelium of individuals with UC (n = 4) compared with controls (n = 5). (D) Representative histograms of HLA-DP expression in EpCAM⁺ epithelial cells in organoids derived from controls or individuals with UC on stimulation with IFN-gamma (100 U/mL) and TNF (20 ng/mL) for the indicated time points measured by flow cytometry (left panel). Plot shows MFI of HLA-DP on IECs in intestinal organoids of controls (n = 8) and individuals with UC (n = 3) on IFN-gamma and TNF stimulation (right panel). All boxes indicate medians with 25% and 75% quartile ranges and whiskers indicate minimum and maximum values. Statistical significance was measured using Mann-Whitney U comparisons.



results in the down-regulation of NKp44 receptor expression on NK cells.

To determine whether NKp44 expression by NK cells as a reflection of activation was also altered in the intestines of individuals with UC, we compared the frequencies and total numbers per cm² of tissue of NKp44⁺ CD56⁺ CD127⁻ NK cells in UC affected intestinal epithelium and controls using flow cytometry. Although frequencies and total numbers of CD56⁺ NK cells did not differ significantly between individuals with UC and controls (data not shown), frequencies of NKp44⁺ cells within CD56⁺ NK cell population and total numbers of NKp44⁺ CD56⁺ CD127⁻ NK cells were significantly lower in intestinal samples from individuals with UC compared with controls (Figure 3B and Supplementary Figure 5C). Due to the relatively small sample size for these in-depth functional studies of intestinal samples, the analyses could not be stratified by *HLA-DP* haplotype. We did, however, observe a negative trend between NKp44⁺ NK cells and HLA-DP⁺ IECs (Spearman $\rho = -0.38$; $P = .2$) assessed on the same sample, suggesting that increased frequencies of HLA-DP⁺ IECs correlate with a decrease in frequencies of intestinal NKp44⁺ NK cells (Supplementary Figure 5D).

In addition to NK cells, epithelial ILCs can express NKp44 and have been shown to contribute to intestinal tissue inflammation.^{16,17,42} To assess whether ILCs also can be activated by HLA-DP molecules in a haplotype-specific manner, sorted intestinal ILCs were incubated with HLA-DP401 or HLA-DP301 molecules. ILCs incubated with HLA-DP401 molecules exhibited a significantly higher TNF production compared with stimulation with HLA-DP301 molecules (Supplementary Figure 5E), whereas IL-22 production was absent on co-incubation with both HLA-DP molecules (data not shown). These observations suggest that the NKp44–HLA-DP receptor–ligand interaction can be used by different immune cell types; however, considering the 12-fold higher numbers of epithelial NKp44⁺ NK cells compared with NKp44⁺ ILCs (Supplementary Figure 5F), NK cells are likely the principal mediators of inflammation in response to HLA-DP expressing IECs.

We next quantified messenger RNA expression of NKp44 (*NCR2*) in single NK cells isolated from the epithelium of UC-affected intestines and controls, as messenger RNA levels should not be affected by engagement with the ligand HLA-DP. *NCR2* was higher expressed in epithelial NK cells from UC-affected epithelium compared with controls (Supplementary Figure 6A). Furthermore, significantly

increased expression of *IFNG*, *LAMP1* (encoding CD107a) and *PRF1* (encoding perforin) was detected in UC-derived epithelial NK cells compared with controls (Supplementary Figure 6A). The percentage of TNF⁺ NK cells did not differ significantly between UC- and control-derived samples (Supplementary Figure 6B), this is in line with previous studies reporting that increased TNF protein levels depend substantially on post-transcriptional regulation.^{28,43,44} Taken together, UC-derived epithelial NK cells have an increased pro-inflammatory profile, together with increased expression of messenger RNA of NKp44. To further visualize the anatomic location of NK cells in the intestinal epithelium, a co-staining using immunofluorescence analysis of CD56 and HLA-DP was established. In line with immunohistochemical and flow cytometric analyses, HLA-DP expression was increased in UC-affected intestines and NK cells were detected neighboring HLA-DP⁺ IECs (Figure 3C, Supplementary Figure 6C and D). Taken together, these data demonstrate the NKp44-expressing NK cells from individuals with UC can be activated and produce pro-inflammatory cytokines upon recognition of HLA-DP401, the *HLA-DP* haplotype associated with UC risk, but not by HLA-DP301, which is associated with a reduced risk of UC.

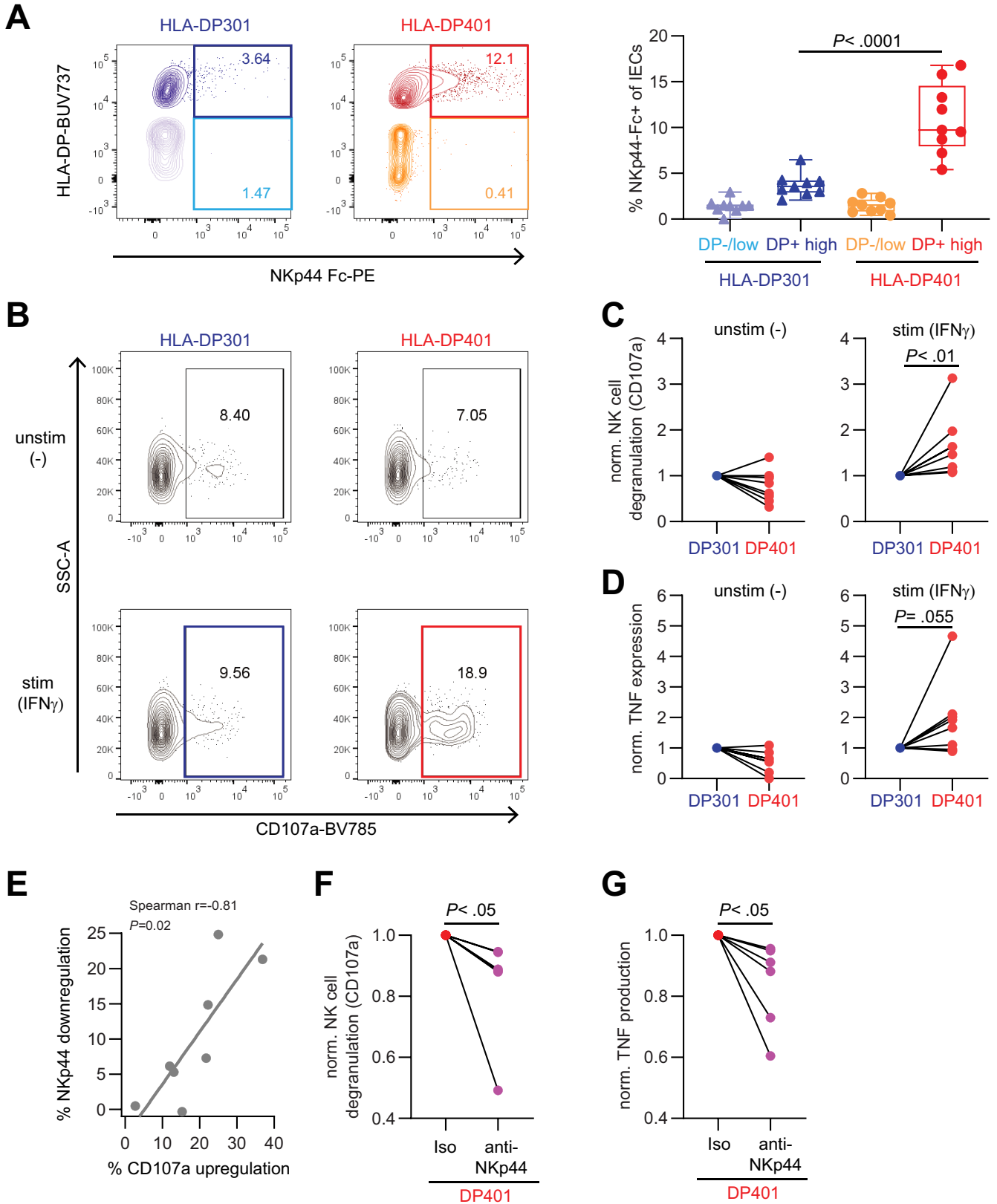
Binding to HLA-DP–Expressing Intestinal Epithelial Cells Results in Increased Activation of Primary NKp44⁺ Natural Killer Cells

To determine whether HLA-DP molecules expressed on IECs can bind to NKp44 and modulate NK cell functioning in a haplotype-dependent manner, we compared binding of NKp44 Fc constructs to IECs in IFN-gamma-stimulated intestinal organoids from *HLA-DP401*^{pos} individuals to organoids from *HLA-DP301*^{pos} individuals. HLA-DP401-expressing IECs displayed significantly higher binding to NKp44 Fc constructs compared with HLA-DP301-expressing IECs (Figure 4A and Supplementary Figure 7A). In contrast, IFN-gamma-treated HLA-DP negative or low-expressing IECs showed no detectable binding to NKp44 Fc constructs, independent of the *HLA-DP* allotype (Figure 4A). In order to investigate whether the differential binding efficiencies of HLA-DP401 and -DP301 to NKp44 resulted in functional consequences for NK cell activation, we quantified CD107a expression of NK cells after coculture with IECs from unstimulated and IFN-gamma-stimulated intestinal organoids from homozygous *HLA-DP401*^{pos} or

Figure 3. Increased activation and TNF production by NK cells of individuals with UC after engagement with HLA-DP401. (A) Representative flow plots for CD107a and TNF, representative histograms of NKp44 expression and summarized plots of peripheral blood-derived NK cells from controls and individuals with UC after incubation with phosphate-buffered saline, HLA-DP301, and HLA-DP401 measured by flow cytometry. Each dot represents an individual donor and lines connect CD107a, TNF, or NKp44 expression of 1 donor (ctrl: n = 9 replicates of 5 donors; UC: n = 8 replicates of 4 donors). (B) Representative histograms of NKp44 expression on intestinal CD56⁺ NK cells in colon of non-inflammatory controls (ctrl) and individuals with UC (left panel) measured by flow cytometry. Median percentages of NKp44⁺ cells of CD56⁺ NK cells in non-inflammatory controls (n = 7) and individuals with UC (n = 6) (middle panel). Median counts of NKp44⁺ CD56⁺ NK cells per cm² in control (n = 7) and UC-affected tissues (n = 6) (right panel). (C) Representative single and merged fluorescence images of HLA-DP, CD56, and 4',6-diamidino-2-phenylindole (DAPI) of control and UC-affected colon tissues. Scale bars: 20 μ m. All boxes indicate medians with 25% and 75% quartile ranges and whiskers indicate minimum and maximum values. Statistical significance was measured using Wilcoxon signed-rank tests (A) or Mann-Whitney U comparisons (B).

-DP301^{pos} individuals (Figure 4B). NK cell donors were matched to organoid donors with regard to their *HLA class I* genotype (*HLA-B/HLA-C*), which was comparable between

HLA-DP401^{pos} and *HLA-DP301^{pos}* donors, and the same NK cell donors were used in coculture experiments with IECs from *HLA-DP401*- and *HLA-DP301*-expressing intestinal



organoids. As described previously,⁴¹ NKp44 expression was highest on CD56⁺⁺ NK cells, allowing interactions with HLA-DP. Therefore, NK cell activation was determined on CD56⁺⁺ NK cells. To adjust for differential expression of NKp44 between different NK cell donors (NKp44⁺ cells of CD56⁺⁺ NK cells ranged from 60% to 90% [data not shown]), degranulation of CD56⁺⁺ NK cells in response to culture with HLA-DP301-expressing IECs was set to 1 for each NK cell donor and compared with NK cell degranulation after coculture with HLA-DP401-expressing IECs. Degranulation did not differ significantly after coculture with unstimulated organoids from either *HLA-DP* haplotypes, but was significantly higher in CD56⁺⁺ NK cells after coculture with IFN-gamma-stimulated, HLA-DP401-expressing IECs compared with coculture with IFN-gamma-stimulated, HLA-DP301-expressing IECs (Figure 4B and C and Supplementary Figure 7B). In line, a trend towards higher TNF production by CD56⁺⁺ NK cells after coculture with IFN-gamma-treated, HLA-DP401-expressing IECs was observed compared with cultures with HLA-DP301-expressing IECs (Figure 4D, Supplementary Figure 7C). As expected, NK cell degranulation was associated with NKp44 down-regulation on CD56⁺⁺ NK cells cocultured with HLA-DP401 expressing IECs (Figure 4E, Spearman ρ : 0.81, P = .02). NK cell degranulation and TNF production in NK cell-IEC (*HLA-DP401*⁺) cocultures was significantly reduced by an anti-NKp44 blocking antibody, further validating the critical interaction of NKp44 with HLA-DP (Figure 4F and G).

To assess whether the enhanced NK cell activation in response to HLA-DP401-expressing IECs resulted in epithelial damage, we performed cocultures of NK cells with intestinal 3D organoids. After 6 hours, the size of HLA-DP401-expressing intestinal 3D-organoids cocultured with CD56⁺⁺ NK cells was reduced significantly, indicating destruction of the 3D organoids by the NKp44⁺ NK cells (Figure 5A), whereas the size of HLA-DP301-expressing organoids in coculture with CD56⁺⁺ NK cells remained similar to cultures without NK cells (Figure 5A). In line with these morphometric analyses, the percentages of dead IECs

in HLA-DP401-expressing organoids cultured with NK cells were significantly higher compared with HLA-DP301-expressing organoids (Figure 5B, Supplementary Figure 8A). Blocking of the NKp44-HLA-DP interaction using an anti-NKp44 blocking antibody rescued viability of HLA-DP401-expressing IECs in organoids cultured with NK cells (Figure 5C). These findings demonstrate that NKp44⁺ NK cells are activated by IECs expressing UC risk HLA-DP401 molecules, resulting in intestinal epithelial tissue damage that can be blocked by anti-NKp44.

Discussion

A combination of microbiota, environmental components, host genetic factors, and mucosal immune dysregulation are involved in the pathogenesis of UC.⁵ In particular, significant genetic associations with UC have been identified in the HLA class II region.^{9,45} Here, we identify *HLA-DPA1*01:03-DPB1*04:01* (HLA-DP401) as a risk haplotype for UC and demonstrate that HLA-DP401 molecules expressed by IECs trigger activation of primary human NK cells via NKp44 resulting in IEC cell death.

Previous studies have identified *HLA-DP* alleles as risk factors for UC.^{9,24} We extended our study to investigate the associations of UC with the *HLA-DP* haplotype, which includes the combination of the α (*HLA-DPA1*) and β (*HLA-DPB1*) chain. These new findings are in line with previous studies reporting a decreased risk of *HLA-DPB1*03:01* and **11:01* alleles and **04:01* with increased risk for UC.⁹ Goyette et al⁹ also identified the *HLA-DPB*06:01* allele to be associated with a decreased risk for UC, which, in our analysis, only showed a trend (P = .09, odds ratio, 0.9), potentially due to differential imputation accuracy score used. Of note, the UC risk allele *HLA-DPB1*04:01* is in weak linkage disequilibrium with the previously reported UC risk HLA class II alleles *HLA-DRB1*15:01*, *HLA-DQA1*01:02*, and *HLA-DQB1*06:01/2*, whereas the UC protective alleles *HLA-DP*11:01* and *HLA-DP*03:01* are in weak linkage disequilibrium with other reported UC protective alleles

Figure 4. Expression of HLA-DP401 on IECs is recognized by NK cells and results in NK cell activation. (A) Representative flow cytometric plots of NKp44 Fc construct binding to HLA-DP301- or HLA-DP401-expressing IECs in organoids after IFN-gamma stimulation (200 U/mL for 3 days) (left panel). Median percentages of NKp44 Fc construct binding to HLA-DP^{low} or HLA-DP^{high} IECs (n = 9 replicates of 2 donors in 3 independent experiments for each haplotype) (right panel). (B) Representative flow cytometric plots showing CD107a expression of CD56⁺⁺ NK cells after coculture with HLA-DP301- or HLA-DP401-expressing IECs. IECs were either unstimulated (-) or stimulated (IFN-gamma) (200 U/mL for 3 days). (C) Plots show fold change degranulation of CD56⁺⁺ NK cells after coculture with unstimulated (-) (left panel) or stimulated (IFN-gamma) (right panel) IECs (degranulation on culture with HLA-DP301-expressing IECs was set to 1 for each NK cell donor). Each dot represents an individual donor (n = 8 NK cell donors) and lines connect CD107a expression of 1 NK cell donor. (D) Plots show fold-change of TNF expression of CD56⁺⁺ NK cells after coculture with unstimulated (-) (left panel) or stimulated (IFN-gamma) (right panel) IECs (TNF expression on culture with HLA-DP301-expressing IECs was set to 1 for each NK cell donor). Each dot represents an individual donor (n = 8 NK cell donors) and lines connect TNF expression of 1 NK cell donor. (E) Plot showing correlation between percentage of NKp44 down-regulation against percentage of CD107 up-regulation on NK cells cocultured with HLA-DP401-expressing IECs (n = 8 NK cell donors). Line indicates linear regression. (F, G) Plots show fold-change degranulation (F) and TNF expression (G) of CD56⁺⁺ NK cells after coculture with IFN-gamma-stimulated HLA-DP401⁺ IECs in presence of an isotype or anti-NKp44 blocking antibody (degranulation and TNF expression of CD56⁺⁺ NK cells upon coculture with HLA-DP401-expressing IECs in presence of an isotype antibody was set to 1 for each NK cell donor). Each dot represents an individual donor (n = 6 NK cell donors) and lines connect CD107a or TNF expression of 1 NK cell donor. All boxes indicate medians with 25% and 75% quartile ranges, and whiskers indicate minimum and maximum values. Statistical significance was measured using Mann-Whitney U comparisons (A) or Wilcoxon signed rank tests (C, D, F, and G).

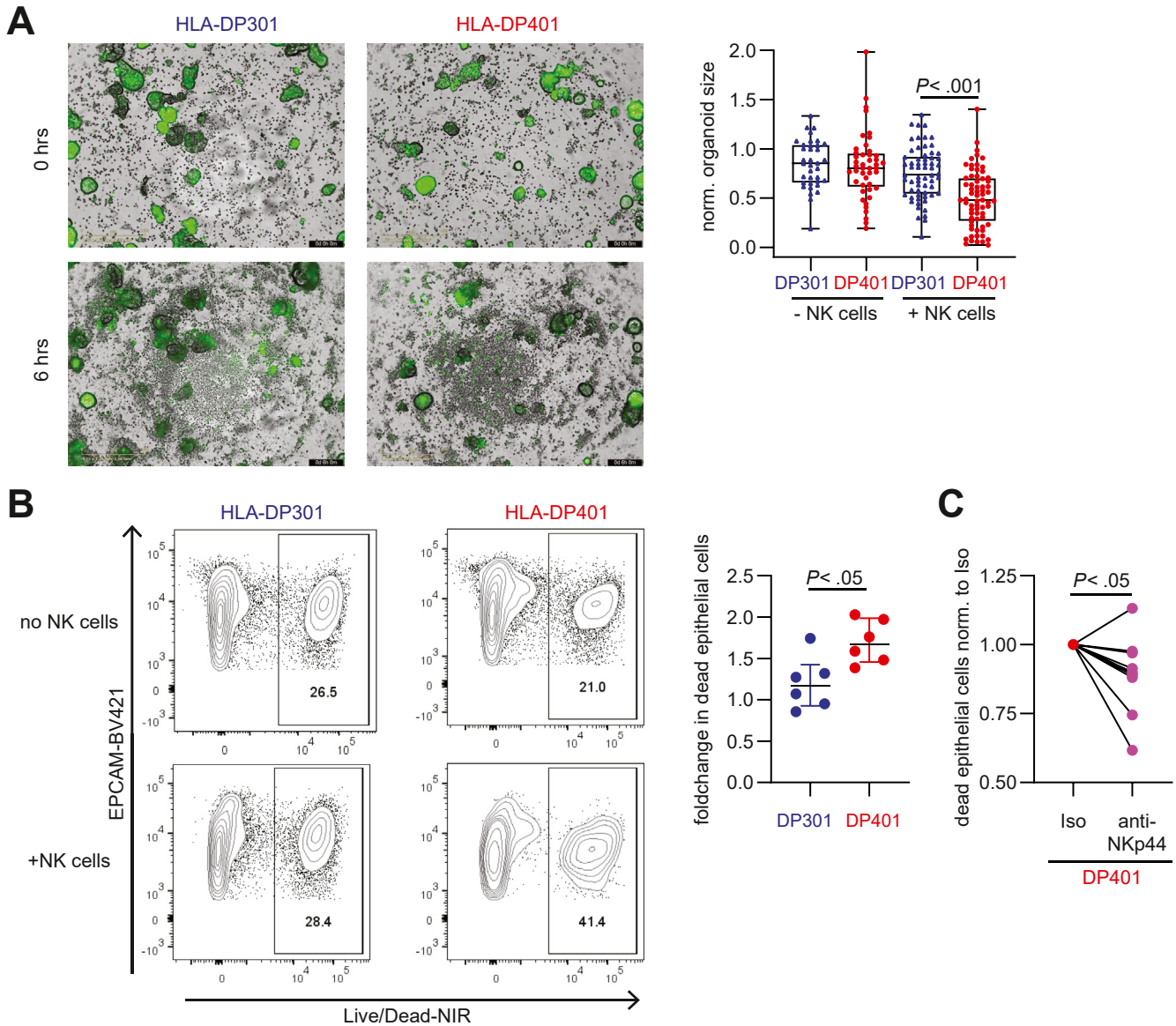


Figure 5. Expression of HLA-DP401 on IECs results in the induction of cytotoxicity by NK cells and reduces IECs viability. (A) Representative *images* of cocultures of CD56⁺⁺ NK cells with IFN- γ -stimulated, calcein-labeled (green) HLA-DP301- or HLA-DP401-expressing intestinal organoids at 0 hours and 6 hours (*left panel*). *Plot* shows normalized organoid size of HLA-DP301- and HLA-DP401-expressing intestinal organoids in presence or absence of CD56⁺⁺ NK cells (n = 36–68 organoids per condition from experiments with 3 different NK cell donors). *Scale bars*: 400 μ m. (B) Representative flow cytometric *plots* showing LIVE/DEAD Fixable Near-IR Dead Cell Stain of HLA-DP301⁺ or HLA-DP401⁺ EpCam⁺ IECs after incubation without NK cells or after coculture with CD56⁺⁺ NK cells. *Plot* shows fold-change (normalized to dead IECs; LIVE/DEAD Fixable Near-IR Dead Cell Stain without NK cells) in dead HLA-DP301⁺ or HLA-DP401⁺ IECs after coculture with CD56⁺⁺ NK cells (n = 6 replicates from 2 NK cell donors). (C) *Plot* shows fold-change in dead HLA-DP401⁺ IECs (LIVE/DEAD Fixable Near-IR Dead Cell Stain) after coculture with CD56⁺⁺ NK cells in presence of an isotype or anti-NKp44 blocking antibody (percentage of dead IECs on culture with CD56⁺⁺ NK cells in presence of an isotype antibody was set to 1 for each NK cell donor). Each *dot* represents an individual donor (n = 10 replicates from 5 NK cell donors) and lines connect 1 NK cell donor. All *boxes* indicate medians with 25% and 75% quartile ranges and *whiskers* indicate minimum and maximum values. Statistical significance was measured using ordinary 2-way analysis of variance (A), Mann-Whitney U comparisons (B), or Wilcoxon signed rank tests (C).

(HLA-DRB1*13:02, HLA-DRB1*07:01, HLA-DQA1*02:01, HLA-DQB1*02:01, and HLA-DQB1*06:04).^{9,24,46,47} We furthermore assessed whether binding of other NK cell receptors, such as LAG-3, to HLA class II molecules³⁴ display distinct patterns associated with UC risk or protective alleles, however, these

were not detected. The findings presented here highlight the need to determine the functional consequences of risk-associated haplotypes in the interactions between human immune and human tissue cells to disentangle the individual contributions of risk alleles and haplotypes in disease

pathogenesis. This is particularly critical for receptors and their ligands, such as NKp44 and HLA-DP, which are restricted to humans and cannot be studied in mice.

Although it is well-known that HLA class II molecules are expressed on antigen-presenting cells and B cells, epithelial cells can induce HLA class II molecule expression upon stimulation with inflammatory signals, through the activation of the transcription factor class II transactivator.^{48,49} In line with previous studies investigating HLA class II molecule expression in UC-affected intestines,^{50,51} we observed significant up-regulation of HLA-DP molecules in the intestinal epithelium of individuals with UC. Stimulation of intestinal organoids with the pro-inflammatory cytokines IFN-gamma and TNF, which also displayed increased expression in UC affected intestinal epithelium, induced HLA-DP up-regulation on IECs, recapitulating the in vivo situation. Organoids generated from *HLA-DP401^{pos}* compared with *HLA-DP301^{pos}* individuals provided the opportunity to demonstrate that IFN-gamma-induced HLA-DP molecules on IECs are recognized by NKp44 in a haplotype-dependent manner, with UC risk HLA-DP401 molecules being recognized by NKp44, while UC-protective HLA-DP301 molecules were not. Interestingly, we also observed higher HLA-DP expression on IFN-gamma and TNF stimulation in intestinal organoids derived from individuals with UC than from controls, indicating that inflammatory response signatures may be maintained in vitro in intestinal organoids. Thus, organoids recapitulate disease states and can be used to investigate the role of specific genotypes in interactions with immune cells in human diseases, especially in the context of genes restricted to humans.⁵²

The role of NK cells in UC has been less investigated compared with other immune cells. This may be due to the molecular differences between human NK cells and those of animal models, especially critical receptors for NK cell functioning, such as killer immunoglobulin-like receptors but also NKp44. Nevertheless, previous studies analyzing human samples have indicated a potential role for NK cells in UC.^{13–15} Here, we show that human NKp44⁺ NK cells were significantly stronger activated by IECs expressing the UC risk molecule HLA-DP401 than by IECs expressing the UC protective molecule HLA-DP301; an observation that is consistent with the better binding of NKp44 to HLA-DP401 compared with HLA-DP301.¹⁸ NK cells have exceptional cytotoxic activity, and these new findings indicate that NKp44⁺ NK cells can induce epithelial tissue damage in UC in an *HLA-DP* haplotype-dependent manner, following the risk profile of our large genetic study. Blocking of NKp44 inhibited NK cell activation and rescued IEC viability in HLA-DP401-expressing organoids confirming the critical role of NKp44 in HLA-DP401-mediated NK cell activation. NKp44 can also be expressed by ILCs, and in line with previous studies NKp44-mediated activation of ILCs influenced production of TNF, but not IL-22, potentially contributing to inflammation and tissue damage in UC.¹⁶ Overall, the methodological approach applied here, using organoid systems encoding for specific HLA alleles, offers a novel in vitro approach to determine interactions of immune cells in immune-mediated diseases in general.

In conclusion, our data identify a molecular and functional immune correlate for the genetic associations of *HLA-DPA1*01:03-DPB1*04:01* and *HLA-DPA1*01:03-DPB1*03:01* in UC by demonstrating *HLA-DP* haplotype-dependent activation of NKp44⁺ NK cells and epithelial tissue damage. Blockade of NKp44/*HLA-DP* interactions might therefore provide a promising future therapeutic approach to decrease epithelial damage in patients with UC who carry the UC risk *HLA-DP* haplotype, and could complement current treatment strategies.

Supplementary Material

Note: To access the supplementary material accompanying this article, visit the online version of *Gastroenterology* at www.gastrojournal.org, and at <http://doi.org/10.1053/j.gastro.2023.06.034>.

References

1. Alatab S, Sepanlou SG, Ikuta K, et al. The global, regional, and national burden of inflammatory bowel disease in 195 countries and territories, 1990–2017: a systematic analysis for the Global Burden of Disease Study 2017. *Lancet Gastroenterol Hepatol* 2020;5:17–30.
2. de Boer NKH, Ahuja V, Almer S, et al. Thiopurine therapy in inflammatory bowel diseases: making new friends should not mean losing old ones. *Gastroenterology* 2019;156:11–14.
3. Al-Horani R, Spanudakis E, Hamad B. The market for ulcerative colitis. *Nat Rev Drug Discov* 2022;21:15–16.
4. Panaccione R, Ghosh S, Middleton S, et al. Combination therapy with infliximab and azathioprine is superior to monotherapy with either agent in ulcerative colitis. *Gastroenterology* 2014;146:392–400.e3.
5. Kobayashi T, Siegmund B, Le Berre C, et al. Ulcerative colitis. *Nat Rev Dis Primers* 2020;6:74.
6. Turner JR. Intestinal mucosal barrier function in health and disease. *Nat Rev Immunol* 2009;9(9):799–809.
7. Matts SG. The value of rectal biopsy in the diagnosis of ulcerative colitis. *Q J Med* 1961;393–407.
8. Geboes K, Riddell R, Öst A, et al. A reproducible grading scale for histological assessment of inflammation in ulcerative colitis. *Gut* 2000;47:404–409.
9. Goyette P, Boucher G, Mallon D, et al. High-density mapping of the MHC identifies a shared role for *HLA-DRB1*01:03* in inflammatory bowel diseases and heterozygous advantage in ulcerative colitis. *Nat Genet* 2015;47:172–179.
10. Huang H, Fang M, Jostins L, et al. Fine-mapping inflammatory bowel disease loci to single-variant resolution. *Nature* 2017;547(7662):173–178.
11. Hegazy AN, West NR, Stubbington MJT, et al. Circulating and tissue-resident CD4⁺ T cells with reactivity to intestinal microbiota are abundant in healthy individuals and function is altered during inflammation. *Gastroenterology* 2017;153:1320–1337.e16.
12. Leppkes M, Neurath MF. Cytokines in inflammatory bowel diseases – update 2020. *Pharmacol Res* 2020;158:104835.

13. Hall LJ, Murphy CT, Quinlan A, et al. Natural killer cells protect mice from DSS-induced colitis by regulating neutrophil function via the NKG2A receptor. *Mucosal Immunol* 2013;6:1016–1026.
14. **Jones DC, Edgar RS**, Ahmad T, et al. Killer Ig-like receptor (KIR) genotype and HLA ligand combinations in ulcerative colitis susceptibility. *Genes Immun* 2006;7:576–582.
15. Fathollahi A, Aslani S, Mostafaei S, et al. The role of killer-cell immunoglobulin-like receptor (KIR) genes in susceptibility to inflammatory bowel disease: systematic review and meta-analysis. *Inflamm Res* 2018;67:727–736.
16. **Glatzer T, Killig M**, Meisig J, et al. ROR γ t⁺ innate lymphoid cells acquire a proinflammatory program upon engagement of the activating receptor NKp44. *Immunity* 2013;38:1223–1235.
17. **Bernink JH, Peters CP**, Munneke M, et al. Human type 1 innate lymphoid cells accumulate in inflamed mucosal tissues. *Nat Immunol* 2013;14:221–229.
18. Niehrs A, Garcia-Beltran WF, Norman PJ, et al. A subset of HLA-DP molecules serve as ligands for the natural cytotoxicity receptor NKp44. *Nat Immunol* 2019;20:1129–1137.
19. **Biton M, Haber AL, Rogel N**, et al. T helper cell cytokines modulate intestinal stem cell renewal and differentiation. *Cell* 2018;175:1307–1320.e22.
20. Wiman K, Curman B, Forsum U, et al. Occurrence of Ia antigens on tissues of non-lymphoid origin [13]. *Nature* 1978;276(5689):711–713.
21. Scott H, Solheim BG, Brandtzaeg P, et al. HLA-DR-like antigens in the epithelium of the human small intestine. *Scand J Immunol* 1980;12:77–82.
22. Parr EL, McKenzie IFC. Demonstration of Ia antigens on mouse intestinal epithelial cells by immunoferritin labeling. *Immunogenetics* 1979;8:499–508.
23. Heuberger C, Pott J, Maloy KJ. Why do intestinal epithelial cells express MHC class II? *Immunology* 2021;162:357–367.
24. Degenhardt F, Mayr G, Wendorff M, et al. Transethnic analysis of the human leukocyte antigen region for ulcerative colitis reveals not only shared but also ethnicity-specific disease associations. *Hum Mol Genet* 2021;30:356–369.
25. **Das S, Forer L, Schönherr S**, et al. Next-generation genotype imputation service and methods. *Nat Genet* 2016;48:1284–1287.
26. Schreeder DM, Cannon JP, Wu J, et al. Cutting edge: FcR-like 6 is an MHC class II receptor. *J Immunol* 2010;185:23–27.
27. Schreurs RRCE, Drewniak A, Bakx R, et al. Quantitative comparison of human intestinal mononuclear leukocyte isolation techniques for flow cytometric analyses. *J Immunol Methods* 2017;445:45–52.
28. Schreurs RRCE, Baumdick ME, Sagebiel AF, et al. Human fetal TNF- α -cytokine-producing CD4⁺ effector memory T Cells promote intestinal development and mediate inflammation early in life. *Immunity* 2019;50:462–476.e8.
29. Sato T, Vries RG, Snippert HJ, et al. Single Lgr5 stem cells build crypt-villus structures in vitro without a mesenchymal niche. *Nature* 2009;459:262–265.
30. Sato T, Stange DE, Ferrante M, et al. Long-term expansion of epithelial organoids from human colon, adenoma, adenocarcinoma, and Barrett's epithelium. *Gastroenterology* 2011;141:1762–1772.
31. Zheng X, Shen J, Cox C, et al. HIBAG - HLA genotype imputation with attribute bagging. *Pharmacogenomics J* 2014;14:192–200.
32. Toyoda H, Wang SJ, Yang HY, et al. Distinct associations of HLA class II genes with inflammatory bowel disease. *Gastroenterology* 1993;104:741–748.
33. Stokkers PCF, Reitsma PH, Tytgat GNJ, et al. HLA-DR and -DQ phenotypes in inflammatory bowel disease: a meta-analysis. *Gut* 1999;45.
34. **Baixeras E, Huard B**, Miossec C, et al. Characterization of the lymphocyte activation gene 3-encoded protein. a new ligand for human leukocyte antigen class H antigens. *J Exp Med* 1992;176:327–337.
35. Hollenbach JA, Madbouly A, Gragert L, et al. A combined DPA1~DPB1 amino acid epitope is the primary unit of selection on the HLA-DP heterodimer. *Immunogenetics* 2012;64:559–569.
36. Steimle V, Otten LA, Zufferey M, et al. Complementation cloning of an MHC class II transactivator mutated in hereditary MHC class II deficiency (or bare lymphocyte syndrome). *Cell* 1993;75:135–146.
37. Thelemann C, Eren RO, Coutaz M, et al. Interferon- γ induces expression of MHC class II on intestinal epithelial cells and protects mice from colitis. *PLoS One* 2014;9:e86844.
38. **Wosen JE, Mukhopadhyay D**, MacAubas C, et al. Epithelial MHC class II expression and its role in antigen presentation in the gastrointestinal and respiratory tracts. *Front Immunol* 2018;9:e86844.
39. Meurer T, Arrieta-Bolaños E, Metzling M, et al. Dissecting genetic control of HLA-DPB1 expression and its relation to structural mismatch models in hematopoietic stem cell transplantation. *Front Immunol* 2018;9:2236.
40. **Masilamani M, Peruzzi G**, Borrego F, et al. Endocytosis and intracellular trafficking of human natural killer cell receptors. *Traffic* 2009;10:1735–1744.
41. Barrow AD, Martin CJ, Colonna M. The natural cytotoxicity receptors in health and disease. *Front Immunol* 2019;10:909.
42. **Cella M, Gamini R**, Sécca C, et al. Subsets of ILC3–ILC1-like cells generate a diversity spectrum of innate lymphoid cells in human mucosal tissues. *Nat Immunol* 2019;20:980–991.
43. Brook M, Sully G, Clark AR, et al. Regulation of tumour necrosis factor α mRNA stability by the mitogen-activated protein kinase p38 signalling cascade. *FEBS Lett* 2000;483:57–61.
44. Kotlyarov A, Neininger A, Schubert C, et al. MAPK kinase 2 is essential for LPS-induced TNF- α biosynthesis. *Nat Cell Biol* 1999;1:94–97.
45. **Liu JZ, Van Sommeren S**, Huang H, et al. Association analyses identify 38 susceptibility loci for inflammatory bowel disease and highlight shared genetic risk across populations. *Nat Genet* 2015;47:979–986.
46. Begovich AB, McClure GR, Suraj VC, et al. Polymorphism, recombination, and linkage disequilibrium

- within the HLA class II region. *J Immunol* 1992; 148:249–258.
47. Howell WM, Evans PR, Devereux SA, et al. Absence of strong HLA-DR/DQ-DP linkage disequilibrium in the British and French Canadian Caucasoid populations. *Int J Immunogenet* 1993;20:363–371.
 48. Hershberg RM, Framson PE, Cho DH, et al. Intestinal epithelial cells use two distinct pathways for HLA class II antigen processing. *J Clin Invest* 1997;100:204–215.
 49. Hershberg RM, Cho DH, Youakim A, et al. Highly polarized HLA class II antigen processing and presentation by human intestinal epithelial cells. *J Clin Invest* 1998; 102:792–803.
 50. Horie Y, Chiba M, Iizuka M, et al. Class II (HLA-DR, -DP, and -DQ) antigens on intestinal epithelia in ulcerative colitis, Crohn's disease, colorectal cancer and normal small intestine. *Gastroenterol Jpn* 1990;25.
 51. Horie Y, Chiba M, Suzuki T, et al. Induction of major histocompatibility complex class II antigens on human colonic epithelium by interferon-gamma, tumor necrosis factor-alpha, and interleukin-2. *J Gastroenterol* 1998; 33:39–47.
 52. Jung JM, Ching W, Baumdick ME, et al. KIR3DS1 directs NK cell-mediated protection against human adenovirus infections. *Sci Immunol* 2021;6(63):eabe2942.

Author names in bold designate shared co-first authorship.

Received October 25, 2022. Accepted June 13, 2023.

Correspondence

Address correspondence to: Madeleine J. Bunders, MD, PhD, Section of Regenerative Medicine and Immunology, III. Department of Medicine, University Medical Center Hamburg-Eppendorf, Martinistraße 52, 20251, Hamburg, Germany. e-mail: madeleine.bunders@leibniz-liv.de; ma.bunders@uke.de.

Acknowledgments

The authors would like to thank all donors of intestinal tissues who participated in this study. In addition, the authors thank their colleagues from the Department of General, Visceral and Thoracic Surgery of the University Hospital Hamburg-Eppendorf for the collection of intestinal tissues. The authors also thank Jana Hennessen and Arne Düsedau from the core facility Fluorescence Cytometry at the Leibniz Institute of Virology and the blood donors and coordinators of the Healthy Cohort at the LIV.

The Hamburg Intestinal Tissue Study Group members include: Alaa Akar, Cornelius Flemming, Felix J. Flomm, Markus Flosbach, Julia Jäger, Niklas Jeromin, Johannes M. Jung, Mareike Ohms, Konrad Reinshagen, Johann Rische, Adrian F. Sagebiel, Deborah Sandfort, Fenja L. Steinert, Christian Tomuschat, and Jasmin Wesche.

The authors thank the International Inflammatory Bowel Disease Genetics Consortium for providing access to the haplotype data.

The International Inflammatory Bowel Disease Genetics Consortium members include: Shifteh Abedian, Clara Abraham, Jean-Paul Achkar, Tariq Ahmad, Rudi Alberts, Behrooz Alizadeh, Leila Amininejad, Ashwin N Ananthakrishnan, Vibeke Andersen, Carl A. Anderson, Jane M. Andrews, Vito Annesse, Guy Aumais, Leonard Baidoo, Robert N. Baldassano, Peter A. Bampton, Murray Barclay, Jeffrey C. Barrett, Johannes Bethge, Claire Bewshea, Joshua C. Bis, Alain Bitton, Thelma BK, Gabrielle Boucher, Oliver Brain, Stephan Brand, Steven R. Brant, Jae Hee Cheon, Angela Chew, Judy H. Cho, Isabelle Cleynen, Ariella Cohain, Rachel Cooney, Anthony Croft, Mark J. Daly, Mauro D'Amato, Silvio Danese, Naser Ebrahim Daryani, Lisa Wu Datta, Frauke Degenhardt, Goda Denapiene, Lee A. Denson, Kathy L. Devaney, Olivier Dewit, Renata D'Inca, Hazel E. Drummond, Maria Dubinsky, Richard H. Duerr, Cathryn Edwards, David Ellinghaus, Pierre Ellul, Motohiro Esaki, Jonah Essers, Lynnette R. Ferguson, Eleonora A. Festen, Philip Fleshner, Tim Florin, Denis Franchimont, Andre Franke, Yuta Fuyuno, Richard Geary, Michel Georges, Christian Gieger, Jürgen Glas, Philippe Goyette, Todd Green, Anne M Griffiths, Stephen L. Guthery, Hakon Hakonarson, Jonas Halfvarson, Katherine Hanigan, Talin Haritunians, Ailsa

Hart, Chris Hawkey, Nicholas K. Hayward, Matija Hedl, Paul Henderson, Georgina L. Hold, Myhungee Hong, Xinli Hu, Hailliang Huang, Jean-Pierre Hugot, Ken Y. Hui, Marcin Imielinski, Omid Jazayeri, Laimas Jonaitis, Luke Jostins, Garima Juyal, Ramesh Chandra Juyal, Rahul Kalla, Tom H. Karlsen, Nicholas A. Kennedy, Mohammed Azam Khan, Won Ho Kim, Takanari Kitazono, Gediminas Kiudelis, Michiaki Kubo, Subra Kugathasan, Limas Kupcinskas, Christopher A Lamb, Katrina M de Lange, Anna Latiano, Debby Laukens, Ian C Lawrance, James C. Lee, Charlie W. Lees, Marcis Leja, Nina Lewis, Johan Van Limbergen, Paolo Lionetti, Jimmy Z. Liu, Edouard Louis, Yang Luo, Gillian Mahy, Masoud Mohammad Malekzadeh, Reza Malekzadeh, John Mansfield, Suzie Marriott, Dunecan Massey, Christopher G. Mathew, Toshiyuki Matsui, Dermot P.B. McGovern, Andrea van der Meulen, Vandana Midha, Raquel Milgrom, Samaneh Mirzaei, Mitja Mitrovic, Grant W. Montgomery, Craig Mowat, Christoph Müller, William G. Newman, Aylwin Ng, Siew C. Ng, Sok Meng Evelyn Ng, Susanna Nikolaus, Kaida Ning, Markus Nöthen, Ioannis Oikonomou, David Okou, Timothy R. Orchard, Orazio Palmieri, Miles Parkes, Anne Phillips, Cyriel Y. Ponsioen, Urös Potocnik, Hossein Poustchi, Natalie J. Prescott, Deborah D. Proctor, Graham Radford-Smith, Jean- Francois Rahier, Miguel Regueiro, Walter Reinisch, Florian Rieder, John D. Rioux, Rebecca Roberts, Gerhard Rogler, Richard K. Russell, Jeremy D. Sanderson, Miquel Sans, Jack Satsangi, Eric E. Schadt, Michael Scharl, John Schembri, Stefan Schreiber, L. Philip Schumm, Regan Scott, Mark Seielstad, Tejas Shah, Yashoda Sharma, Mark S. Silverberg, Alison Simmons, Lisa A. Simms, Abhey Singh, Jurgita Skieceviciene, Suzanne van Sommeren, Kyuyoung Song, Ajit Sood, Sarah L. Spain, A. Hillary Steinhart, Joanne M. Stempak, Laura Stronati, Joseph J. Y. Sung, Stephan R. Targan, Kirstin M. Taylor, Emilie Theatre, Leif Torkvist, Esther A. Torres, Mark Tremelling, Holm H. Uhlig, Junji Umeno, Homayon Vahedi, Eric Vasiliauskas, Anje ter Velde, Nicholas T. Venham, Severine Vermeire, Hein W. Verspaget, Martine De Vos, Thomas Walters, Kai Wang, Ming-Hsi Wang, Rinse K. Weersma, Zhi Wei, David Whiteman, Cisca Wijmenga, David C. Wilson, Juliane Winkelmann, Sunny H. Wong, Ramnik J. Xavier, Keiko Yamazaki, Suk-Kyun Yang, Byong Duk Ye, Sebastian Zeissig, Bin Zhang, Clarence K. Zhang, Hu Zhang, Wei Zhang, Hongyu Zhao, Zhen Z. Zhao, Australia and New Zealand Inflammatory Bowel Disease Genetics Consortium, Belgium Inflammatory Bowel Disease Genetics Consortium, Italian Group for Inflammatory Bowel Disease Genetic Consortium, National Institute of Diabetes and Digestive and Kidney Disease Inflammatory Bowel Disease Genetics Consortium, Quebec Inflammatory Bowel Disease Genetics Consortium, United Kingdom Inflammatory Bowel Disease Genetics Consortium, and Wellcome Trust Case Control Consortium.

CrediT Authorship Contributions

Martin Eckard Baumdick, PhD (Data curation: Lead; Formal analysis: Equal; Investigation: Equal; Writing – original draft: Equal; Writing – review & editing: Equal).

Annika Niehrs, PhD (Data curation: Supporting; Formal analysis: Equal; Investigation: Equal; Writing – original draft: Equal; Writing – review & editing: Equal).

Frauke Degenhardt, PhD (Data curation: Supporting; Formal analysis: Supporting; Investigation: Supporting; Writing – review & editing: Supporting).

Maria Schwerk, MSc (Investigation: Supporting; Writing – review & editing: Supporting).

Ole Hinrichs, MSc (Investigation: Supporting; Writing – review & editing: Supporting).

Ana Jordan-Paiz, PhD (Investigation: Supporting; Writing – review & editing: Supporting).

Benedetta Padoan, MSc (Investigation: Supporting; Writing – review & editing: Supporting).

Lucy H. M. Wegner, MD candidate (Investigation: Supporting; Writing – review & editing: Supporting).

Sebastian Schloer, PhD (Investigation: Supporting; Writing – review & editing: Supporting).

Britta F. Zecher, MD (Investigation: Supporting; Writing – review & editing: Supporting).

Jakob Malsy, MD (Investigation: Supporting; Writing – review & editing: Supporting).

Vinita R. Joshi, PhD (Investigation: Supporting; Writing – review & editing: Supporting).

Christin Illig, technical assistant (Investigation: Supporting; Writing – review & editing: Supporting).

Jennifer Schröder-Schwarz, technical assistant (Investigation: Supporting).

Kimberly J. Möller, MD (Investigation: Supporting; Writing – review & editing: Supporting).

Hamburg Intestinal Tissue Study Group (Experiments: Supporting; Writing – review & editing: Supporting).

Maureen Martin, MD (Investigation: Supporting; Writing – review & editing: Supporting).

Yuko Yuki, research associate (Investigation: Supporting; Writing – review & editing: Supporting).

Mikki Ozawa, PhD (Investigation: Supporting; Writing – review & editing: Supporting).

Jurgen Sauter, PhD (Investigation: Supporting; Writing – review & editing: Supporting).

Alexander H. Schmidt, PhD (Investigation: Supporting; Writing – review & editing: Supporting).

Daniel Perez, MD (Investigation: Supporting; Writing – review & editing: Supporting).

Anastasios D. Giannou, MD, PhD (Investigation: Supporting; Writing – review & editing: Supporting).

Mary Carrington, PhD (Investigation: Supporting; Writing – review & editing: Supporting).

Randall S. Davis, MD (Investigation: Supporting; Writing – review & editing: Supporting).

Udo Schumacher, MD (Investigation: Supporting; Writing – review & editing: Supporting).

Guido Sauter, MD (Investigation: Supporting; Writing – review & editing: Supporting).

Samuel Huber, MD (Investigation: Supporting; Writing – review & editing: Supporting).

Victor G. Puelles, MD, PhD (Investigation: Supporting; Writing – review & editing: Supporting).

Nathaniel Melling, MD (Investigation: Supporting; Writing – review & editing: Supporting).

Andre Franke, PhD (Investigation: Supporting; Writing – review & editing: Supporting).

International Inflammatory Bowel Disease Genetics Consortium (Data curation: Supporting).

Marcus Altfeld, MD, PhD (Conceptualization: Equal; Supervision: Equal; Writing – original draft: Equal; Writing – review & editing: Equal).

Madeleine J. Bunders, MD, PhD (Conceptualization: Equal; Supervision: Equal; Writing – original draft: Equal; Writing – review & editing: Equal).

Conflicts of interest

These authors disclose the following: Annika Niehrs and Marcus Altfeld are inventors of 1 provisional patent that describes the binding of NKp44 to a

subset of HLA-DP molecules, and the role of these interactions in graft-versus-host disease. The remaining author disclose no conflicts.

Funding

This work was supported by the Daisy Huet Roell Foundation, the European Research Council (ERC) (EU Horizon 2020, #884830), the Landesforschungsförderung (LFF-75) Hamburg City of Hamburg, the DFG (CRC/1192), the DFG (SFB1328), the BMBF (eMed Consortia Fibromap), and the Novo Nordisk Foundation (Young Investigator Award – NNF21OC0066381). This project has been funded in part with federal funds from the Frederick National Laboratory for Cancer Research, under Contract No. HHSN261200800001E, and by the Intramural Research Program of the National Institutes of Health, Frederick National Laboratory, Center for Cancer Research. The content of this publication does not necessarily reflect the views or policies of the Department of Health and Human Services, nor does mention of trade names, commercial products, or organizations imply endorsement by the US Government. The Leibniz Institute of Virology is supported by the Free and Hanseatic City of Hamburg and the Federal Ministry of Health.

Data Availability

The ImmunoChip data used in this study are proprietary to the International Inflammatory Bowel Disease Genetics Consortium and may be requested from the consortium (<http://www.ibdgenetics.org/>). All other data used in this study have been collected in clinical studies and are subject to the regulations of the ethics committee of the Freie und Hansestadt Hamburg (Ärztammer Hamburg). Participant's written informed consent has been provided for data generation and handling according to the approved protocols and scopes of the study. Data storage is performed at the Leibniz Institute of Virology. Data are available on request and can be shared after confirming that data will be used within the scope of the originally provided informed consent. Further information and requests for data should be directed to the lead contact, Madeleine J. Bunders ([ma.bunders@uke.de](mailto:mbunders@uke.de)).

Supplementary Methods

Imputation and Phasing With the Michigan Imputation Server

Imputation was performed on the Michigan Imputation Server with a multi-ethnic reference panel (version 1.0, 2021; full context HLA panel) published by Luo et al,^{e1} which included 18,293 individuals and 54,474 sites, including amino acid, single nucleotide polymorphism, and HLA allele information. Results were received as a single variant call format file with genotype, genotype dosage, and genotype probability, as well as genotype phase information given for each individual and HLA allele. Using the given phase information, alleles were combined into HLA-DPA1-DPB1 haplotypes at 2-field level based on variant call format file genotype hardcalls using PLINK, version 1.9^{e2} and R version, 3.6.2. Individuals with missing allele information after imposing the above frequency and imputation quality cutoffs, were set to missing for both parental haplotypes. This left 13,717 UC cases and 26,417 controls for analysis. In total 3 two-field HLA-DPA1 and 19 two-field HLA-DPB1 alleles were imputed into the data with an allele frequency >0.5%. All had an imputation score (R^2) > 0.6.

Imputation and Phasing With HLA Genotype Imputation With Attribute Bagging

Imputation and phasing were performed as described in detail previously.^{e3,31} In brief, HLA alleles were imputed for HLA-DPA1 and HLA-DPB1 using HLA genotype imputation with attribute bagging (HIBAG) and multi-ethnic reference panel, containing 1300 individuals at 2-digit full HLA context. Phasing was performed by comparison of single nucleotide polymorphism haplotypes from 10 random out of 100 HIBAG classifiers stored in the HIBAG reference model and single nucleotide polymorphism haplotypes phased using SHAPEIT2. Phasing certainty was determined as the number of congruent phasing results across 10 of the 100 random classifiers. Individuals with HLA genotype imputation quality scores >0.8 for HLA-DPA1 or HLA-DPB1 and a per locus phasing certainty >0.6 were included in the analysis. This left, in total, 13,134 UC cases and 25,248 controls. In total, 4 two-field HLA-DPA1 and 15 two-field HLA-DPB1 alleles were imputed into the data with allele frequency >0.5%. Of these, all had an imputation (marginal probability as calculated in Degenhardt et al²⁴) score > 0.6.

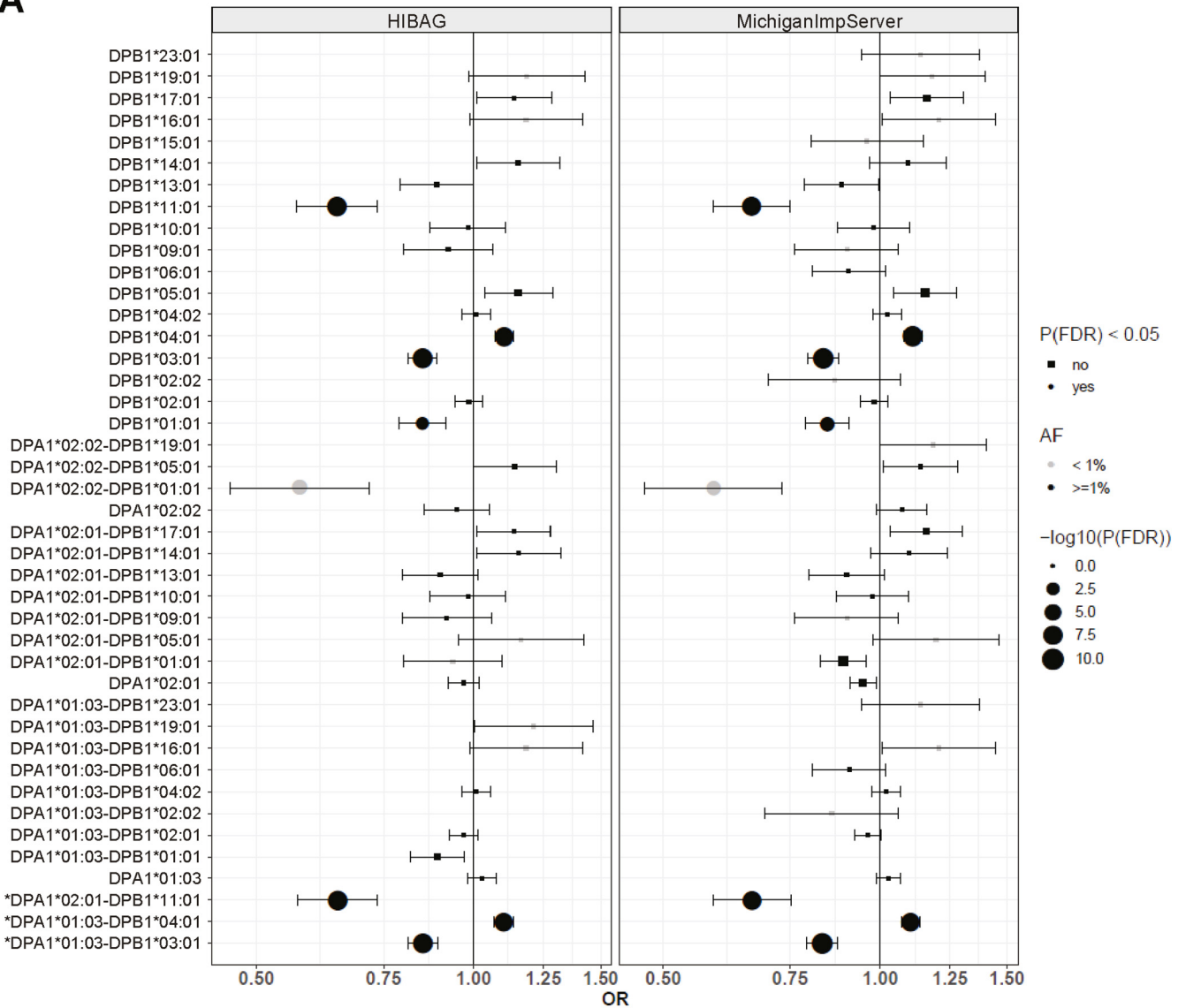
Results of HLA-Haplotype Analysis

The overall correlation between allele frequencies imputed into the data across the imputation with HIBAG and the Michigan Imputation Server was high, with a Pearson correlation coefficient of 0.997. Alleles with strikingly deviating allele frequencies included DPB1*06:01, which had an allele frequency of 1.7% in the data imputed with the Michigan Imputation Server and of <0.5% in the data imputed with HIBAG. This allele had previously been associated with UC.⁹ Here we could not replicate this association ($P = .09$; odds ratio, 0.904; 95% confidence level, .804–1.017), although the genotype data used were nearly identical. In comparison with the imputation score of 0.5 for this allele described previously,⁹ we achieved a higher imputation accuracy score of 0.85 with the multi-ethnic panel,^{e1} which may explain this discrepancy. In addition, we observed deviating frequencies for HLA-DPA1*01:03 and HLA-DPA1*02:01 and haplotypes thereof. We observed during phasing with HIBAG that particularly DPA1*01:03 and DPA1*02:01 were challenging to phase, both alleles being at instances assigned the same phase if they occurred in the same individual. Although DPA1*01:03 had frequencies of 87.1% (imputation score = 1.00) and 82.5% ($R^2 = 0.96$) in the data imputed with HIBAG and the Michigan Imputation Server, respectively, DPA1*02:01 had frequencies of a 10.5% (imputation score = 0.94) and 13.9% ($R^2 = 0.99$). Because both imputation accuracies are high with HIBAG and the Michigan Imputation Server, association analyses on HLA typed DPA1*01:03/DPA1*02:01 should be analyzed in more detail in future studies. This is also true for re-analysis of the association of HLA-DPB1*06:01 with UC.

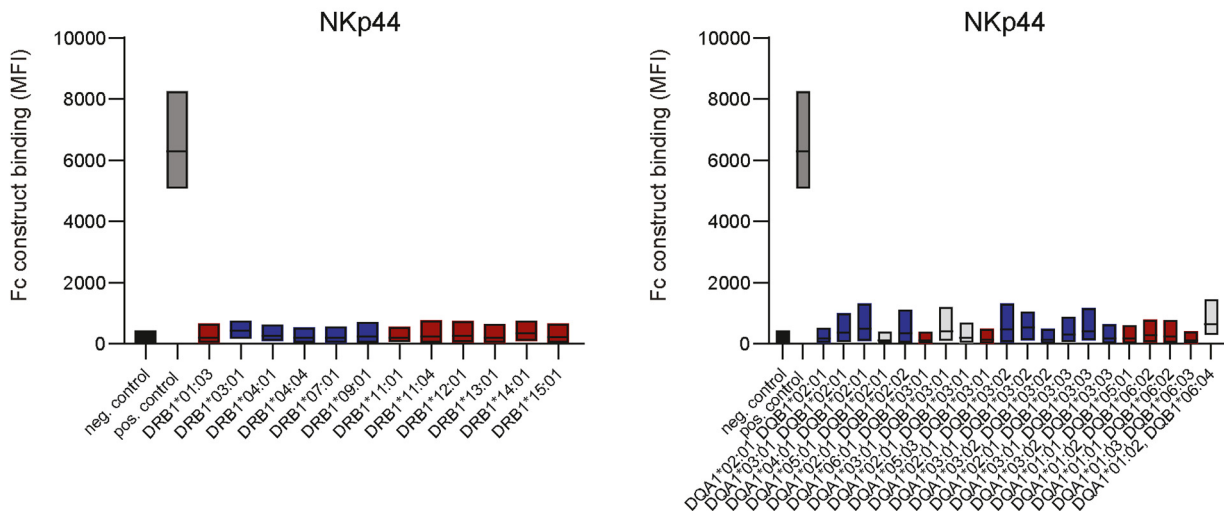
Supplementary References

- e1. Luo Y, Kanai M, Choi W, et al. A high-resolution HLA reference panel capturing global population diversity enables multi-ancestry fine-mapping in HIV host response. *Nat Genet* 2021;53:1504–1516.
- e2. Purcell S, Neale B, Todd-Brown K, et al. PLINK: a tool set for whole-genome association and population-based linkage analyses. *Am J Hum Genet* 2007; 81:559–575.
- e3. Degenhardt F, Wendorff M, Wittig M, et al. Construction and benchmarking of a multi-ethnic reference panel for the imputation of HLA class I and II alleles. *Hum Mol Genet* 2019;28:2078–2092.

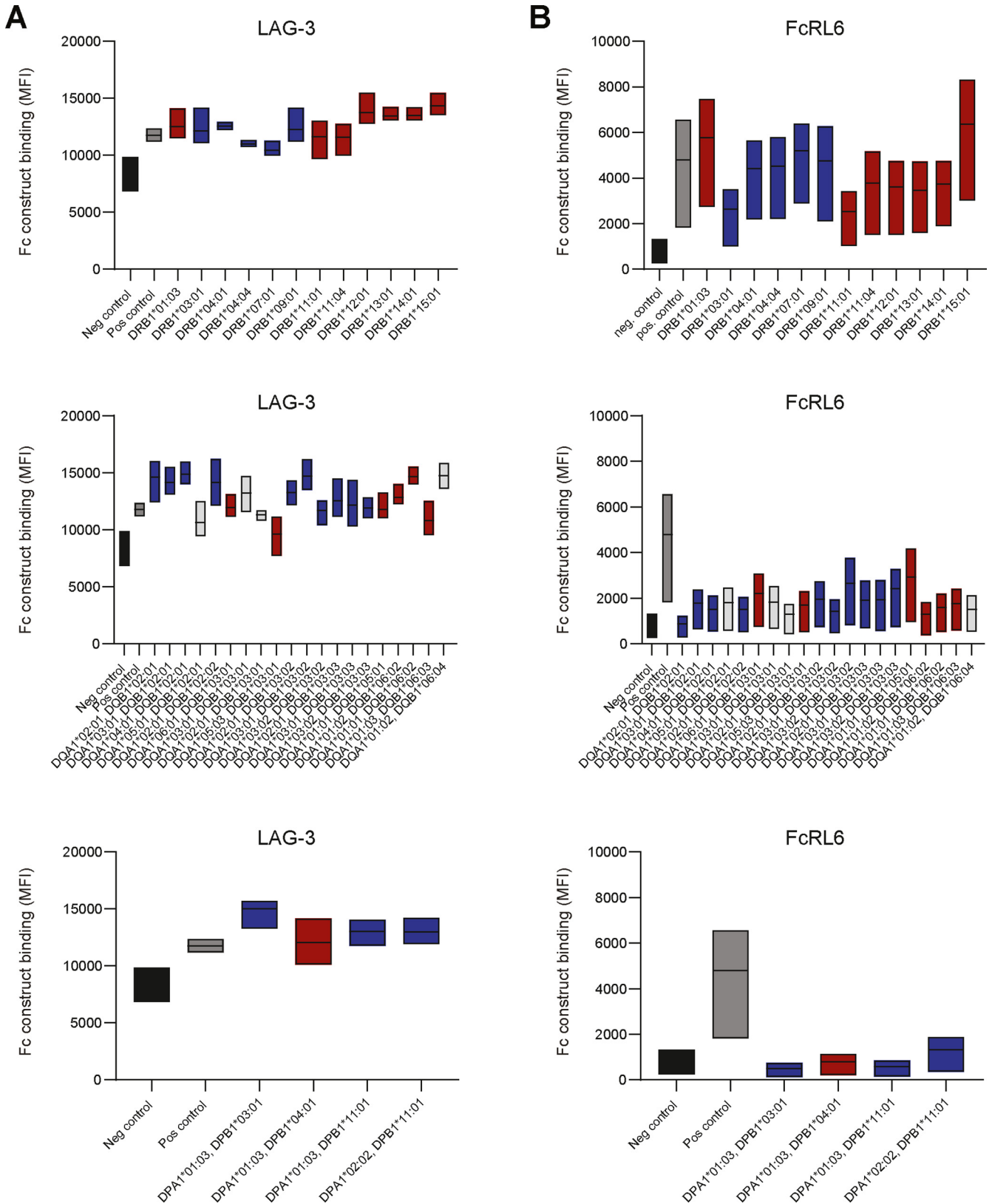
A



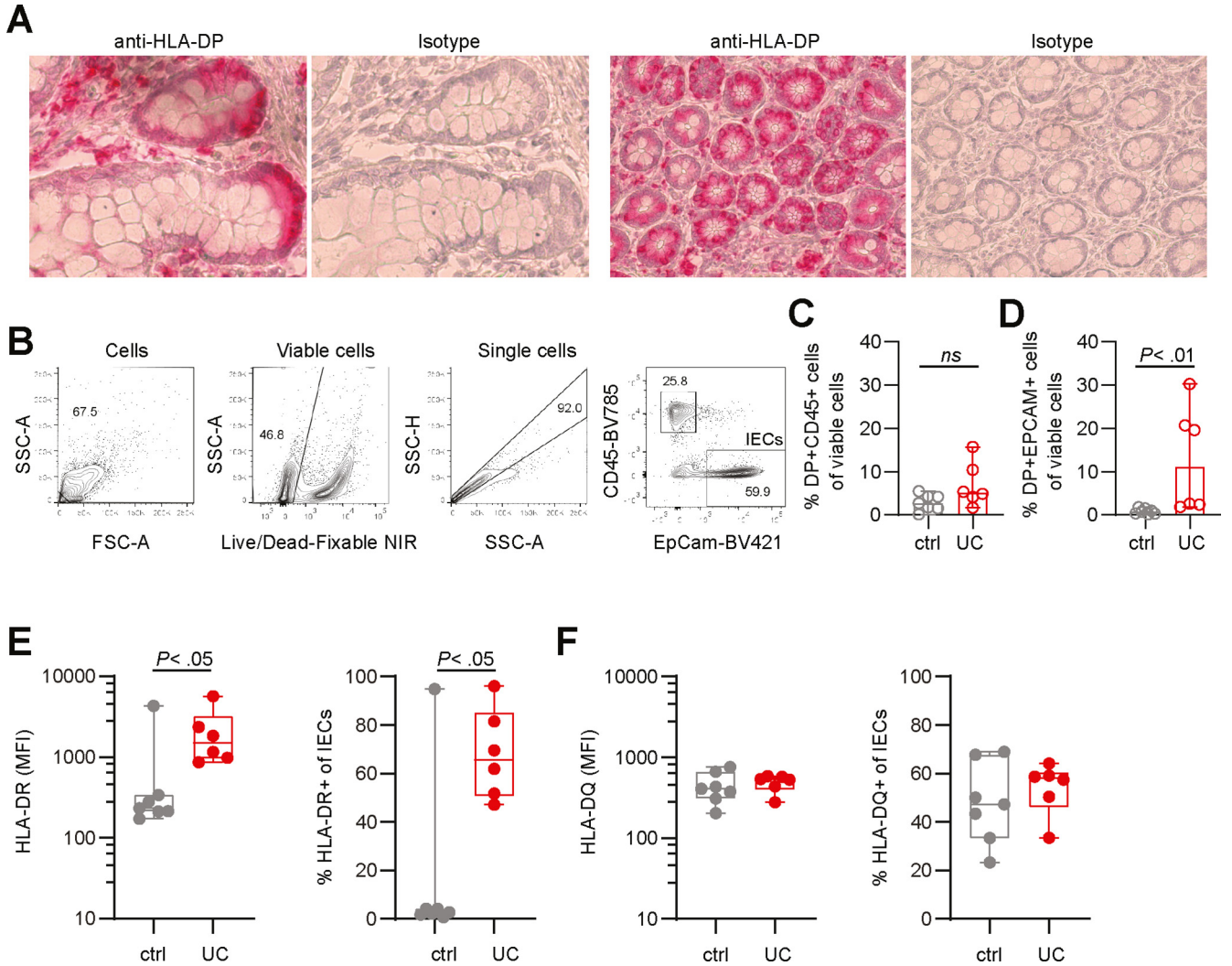
B



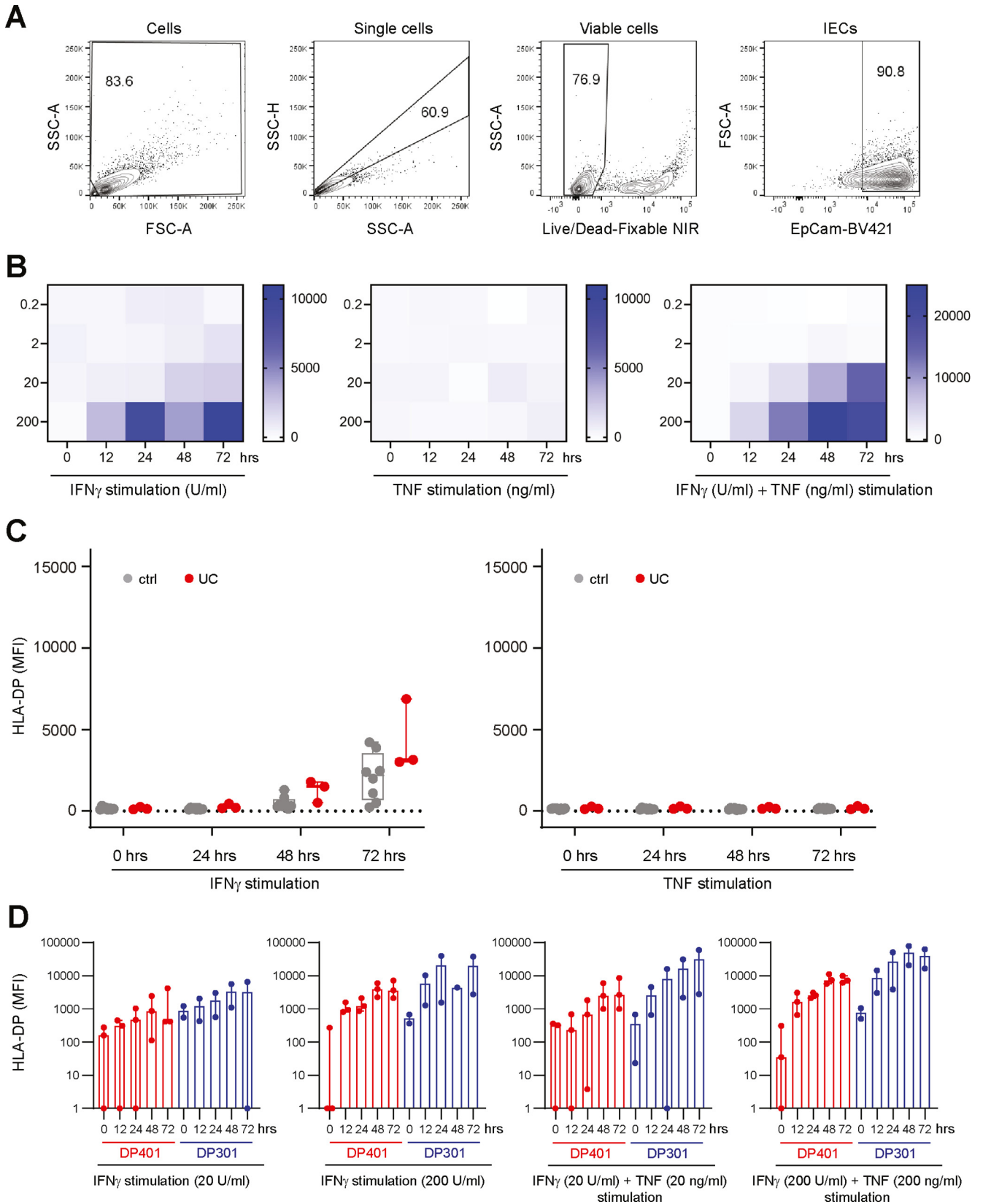
Supplementary Figure 1. Associations of HLA-DPA1 and HLA-DPB1 alleles and HLA-DPA1-DPB1 haplotypes with UC. (A) Imputation of HLA-DPA1-DPB1 haplotypes using HIBAG and Michigan Imputation Server showing UC risk and protective HLA-DPA1/DPB1 alleles and HLA-DPA1-DPB1 haplotypes with their frequencies and false discovery rate *P* values (*P*[FDR]). Odds ratios (OR) and 95% CIs are indicated. (B) NKp44 Fc construct binding to beads coated with different HLA-DR (*left panel*) or HLA-DQ molecules (*right panel*) was determined and medians of fluorescence intensity (MFIs) are depicted (*n* = 6). UC associated risk haplotypes are in *red*, protective haplotypes are in *blue*, haplotype combinations of a risk and a protective allele are in *light gray*. Boxes indicate mean with minimum and maximum MFI of each HLA-DR/DQ molecule tested.



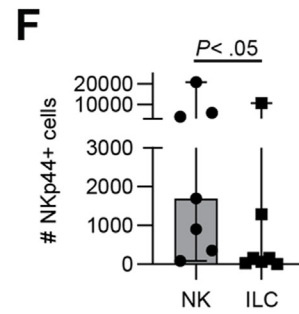
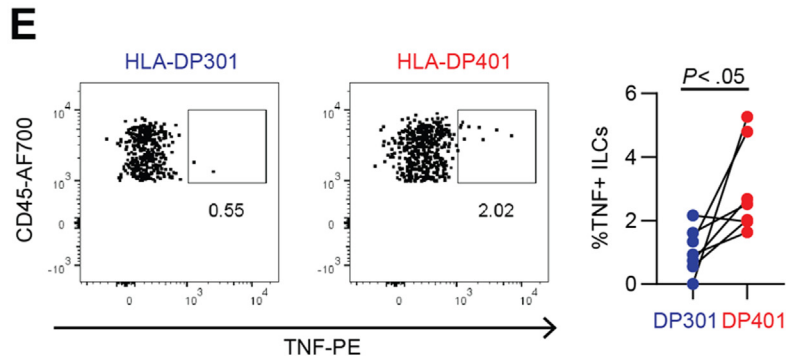
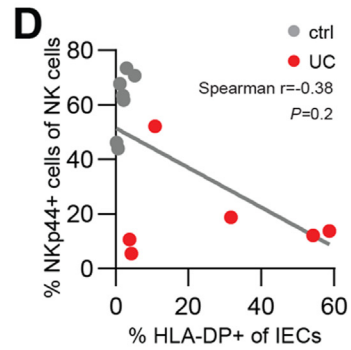
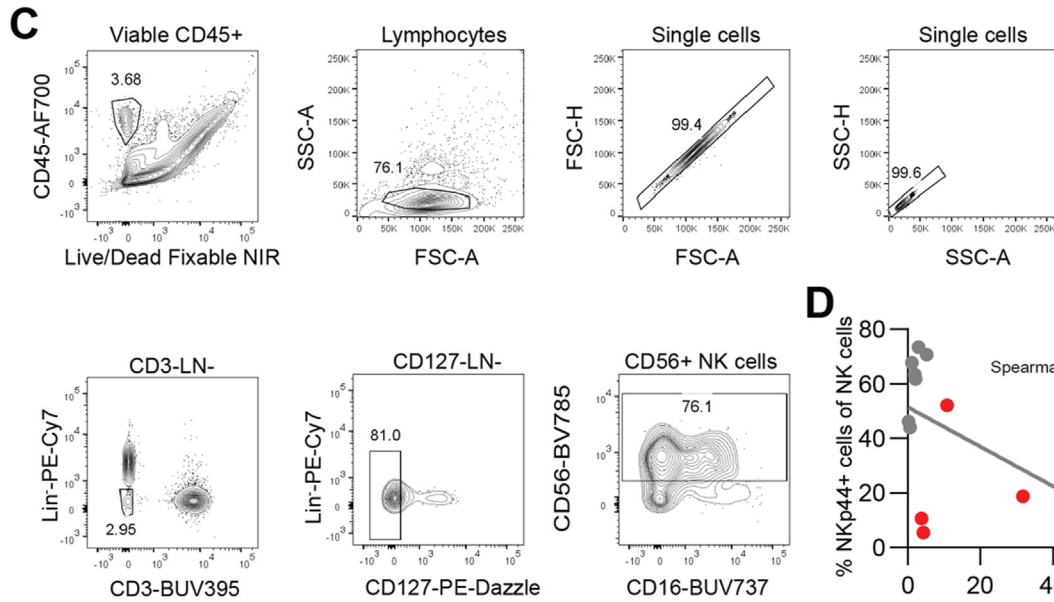
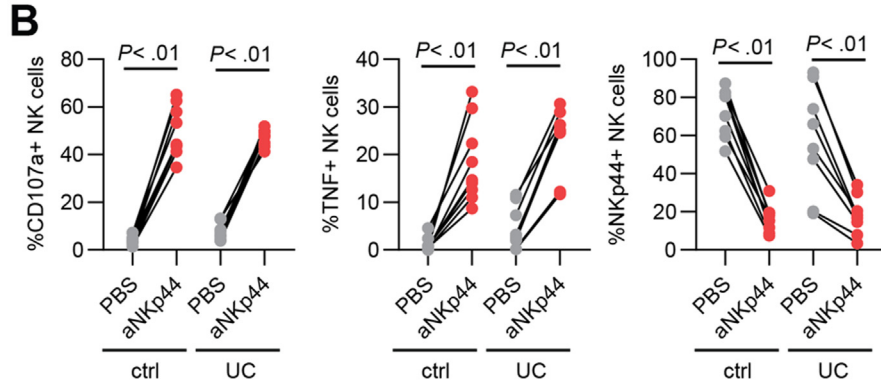
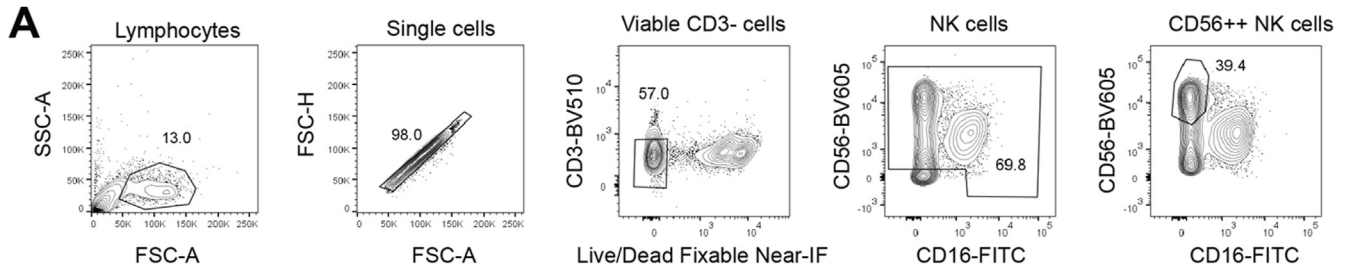
Supplementary Figure 2. HLA-DR, -DQ and -DP binding to LAG-3 and FcRL6. (A, B) LAG-3 Fc construct (A) and FcRL6 Fc construct (B) binding to beads coated with different HLA-DR (upper panel), HLA-DQ (middle panel), or HLA-DP molecules (lower panel) were determined and medians of fluorescence intensity (MFIs) are depicted (n = 3). UC-associated risk haplotypes are in red, protective haplotypes are in blue, haplotype combinations of a risk and a protective allele are in light gray. Boxes indicate mean with minimum and maximum MFI of each HLA-DR/DQ molecule tested.



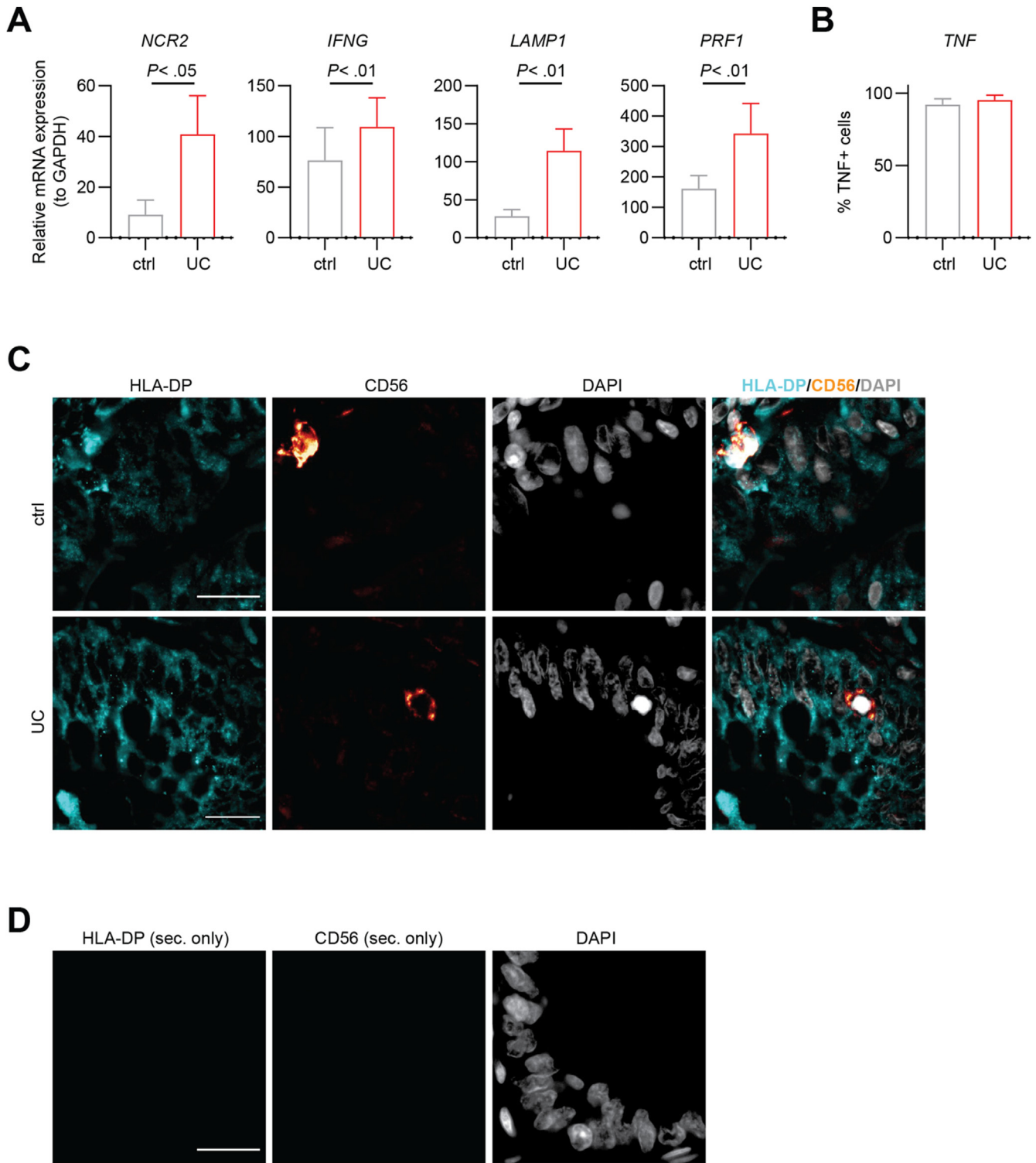
Supplementary Figure 3. HLA class II up-regulation in IECs of individuals with UC. (A) Control *images* of immunohistochemical analyses of UC colon samples. Specific HLA-DP expression is labeled in *red*, hemalum was used as a nuclear counterstain (*blue*). Isotype antibody staining was used as a negative control. (B) Gating strategy to identify IECs (viable CD45⁻EpCam⁺) and lymphocytes (CD45⁺EpCam⁻) derived from intestinal tissue samples. (C, D) Median percentages and interquartile ranges of HLA-DP⁺ CD45⁺ cells (C) or HLA-DP⁺ EpCAM⁺ IECs (D) of all viable cells from controls (n = 7) and patients with UC (n = 6) (*right panel*). (E) Expression of HLA-DR on EpCam⁺ IECs depicted as MFI (*left panel*). Median percentages of HLA-DR⁺ cells of EpCam⁺ IECs of controls (n = 7) and patients with UC (n = 6) (*right panel*). (F) Expression of HLA-DQ on EpCam⁺ IECs depicted as MFI (*left panel*). Median percentages of HLA-DQ⁺ cells of EpCam⁺ IECs of controls (n = 7) and patients with UC (n = 6) (*right panel*). In *panels E and F*, boxes indicate medians with 25% and 75% quartile ranges and *whiskers* indicate minimum and maximum values. Statistical significance was measured using Mann-Whitney U comparisons.



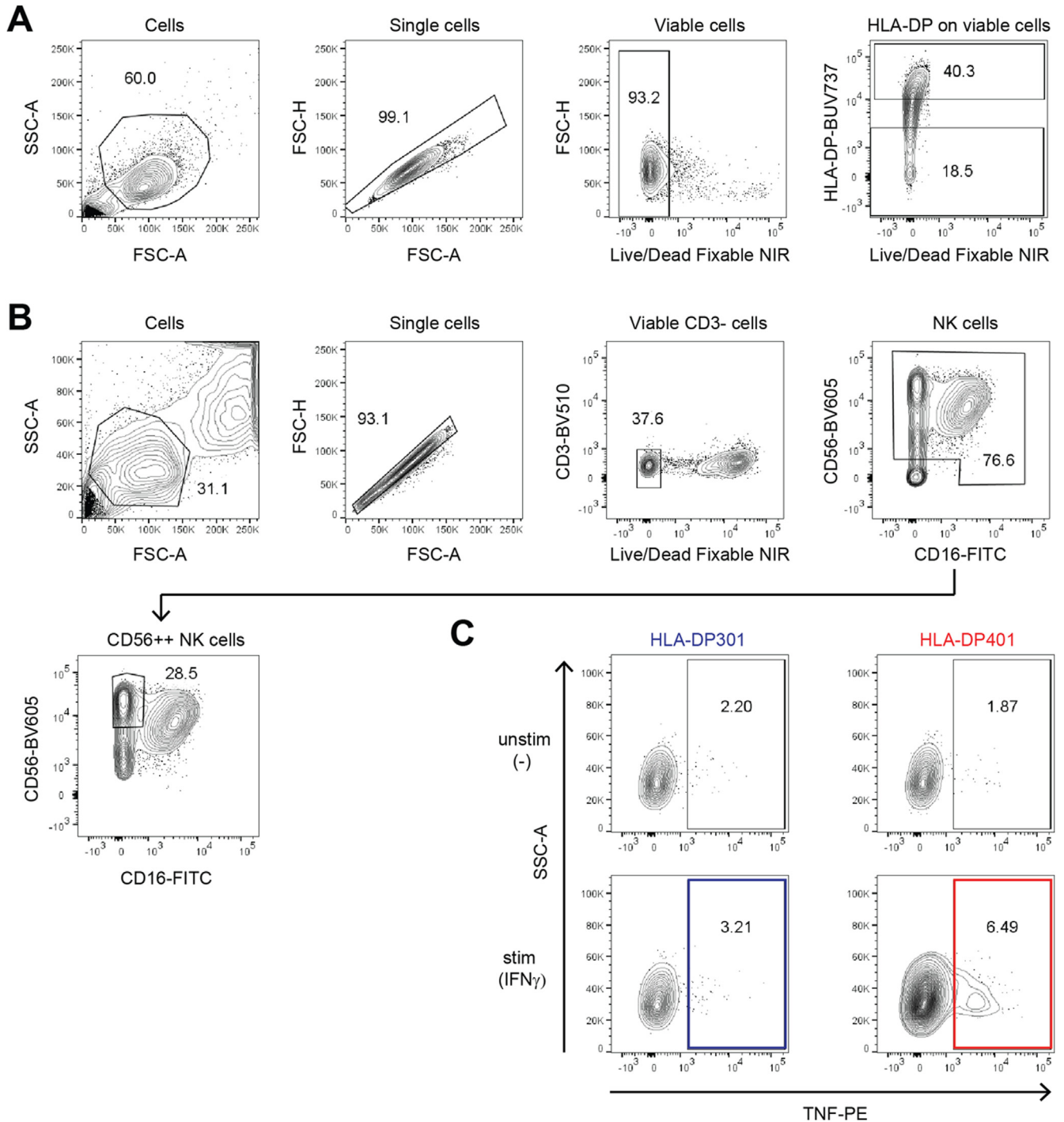
Supplementary Figure 4. IFN-gamma- and TNF-mediated up-regulation of HLA class II in intestinal organoids. (A) Gating strategy to identify (viable EpCam⁺) IECs derived from intestinal organoids. (B) *Heatmaps* showing the MFI of HLA-DP on EpCam⁺ IECs derived from intestinal organoids on stimulation with increasing concentrations of IFN-gamma (U/mL) or TNF (ng/mL) for the indicated time points (n = 5 donors). (C) *Plots* showing MFI of HLA-DP of IECs of control (n = 8) and UC-derived (n = 3) intestinal organoids on IFN-gamma (100 U/mL, *left panel*) or TNF stimulation (20 ng/mL, *right panel*) for the indicated time points. (D) *Plots* showing HLA-DP expression of HLA-DP401⁺ (n = 3) and HLA-DP301⁺ (n = 2) IECs derived from intestinal organoids on IFN-gamma (20 U/mL and 200 U/mL) or stimulation with IFN-gamma and TNF (IFN-gamma: 20 U/mL, TNF: 20 ng/mL or IFN-gamma: 200 U/mL, TNF: 200 ng/mL) for the indicated time points depicted as MFI. In *panel C*, boxes indicate medians with 25% and 75% quartile ranges and *whiskers* indicate minimum and maximum values. Statistical significance was measured using Mann-Whitney U comparisons.



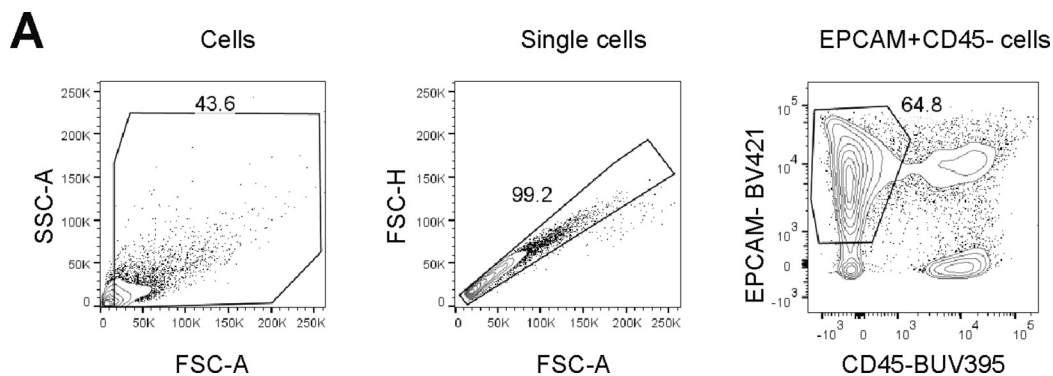
Supplementary Figure 5. Functional responses of NKp44⁺ NK cells and ILCs after ligand engagement. (A) Gating strategy to identify peripheral blood-derived CD56⁺⁺ NK cells. (B) Percentage of CD107a⁺, TNF⁺, or NKp44⁺ NK cells are shown for control (phosphate-buffered saline) and paired stimulated (anti-NKp44) CD56⁺⁺ NK cells (ctrl: n = 9 replicates of 5 donors; UC: n = 8 replicates of 4 donors). (C) Gating strategy for intestinal NK cells. NK cells are defined as viable CD45⁺, lineage⁻ (Lin⁻:CD14⁻, CD19⁻, BDCA2⁻, CD1a⁻, CD123⁻, CD34⁻), CD3⁻, CD127⁻, and CD56⁺ cells. (D) Plot showing correlation between percentages of HLA-DP⁺ IECs and NKp44⁺ NK cells of the same donor (ctrl and UC; n = 13). Line indicates linear regression. (E) Representative flow cytometric plots showing TNF expression of intestinal ILCs after stimulation with HLA-DP301 or HLA-DP401 molecules (left panel). Plot shows percentages of TNF⁺ ILCs (right panel) (n = 7 donors). (F) Median counts and interquartile ranges of epithelial NKp44⁺ NK cells and NKp44⁺ ILCs per cm² (n = 7). Statistical significance was measured using Wilcoxon signed rank (B, E, F).



Supplementary Figure 6. Gene expression of NK cells in intestinal epithelium of individuals with UC and controls. (A) Plots showing mean + SEM of relative messenger RNA expression of *NCR2* (encoding NKp44), *IFNG*, *LAMP1* (encoding CD107a), and *PRF1* (encoding perforin) to reference gene *GAPDH* of single NK cells of controls ($n = 80$ cells of 3 donors) or individuals with UC ($n = 86$ cells of 3 donors). (B) Plot showing mean + SEM of percentages of TNF⁺ NK cells per donor of controls ($n = 3$) and individuals with UC ($n = 3$). (C) Representative single and merged fluorescence images of HLA-DP, CD56, and 4',6-diamidino-2-phenylindole (DAPI) of control and UC-affected colons. (D) Fluorescence images of secondary antibody only staining and DAPI. Scale bars: 20 μ m.



Supplementary Figure 7. TNF production by CD56⁺⁺ NK cells on coculture with HLA-DP401⁺ IECs. (A) Gating strategy to identify IECs derived from intestinal organoids for assessment of NKp44 Fc construct binding. IECs are defined as viable cells and were separated into HLA-DP low (*lower gate*) and high (*upper gate*) expressing IECs. (B) Gating strategy for CD56⁺⁺ NK cells after coculture with IECs derived from intestinal organoids. CD56⁺⁺ NK cells are defined as single, viable, CD3⁻, CD16⁻, CD56⁺⁺ cells. (C) Representative flow cytometric *plots* showing TNF expression of CD56⁺⁺ NK cells after coculture with HLA-DP301- or HLA-DP401-expressing IECs. IECs were either unstimulated (-) or stimulated (IFN- γ) (200 U/mL for 3 days).



Supplementary Figure 8. Gating strategies for IECs. (A) Gating strategy to identify IECs (CD45⁺EpCam⁺) derived from intestinal organoids and assess percentage of viable IECs.

Supplementary Table 1. Donor Characteristics (n = 39)

Characteristic	Data
Sex, n	
Male	17
Female	22
Age at surgery, y, median (interquartile range)	57 (41–65)
Primary diagnosis, n	
Malignancy	25
UC	12
Other	2
Indication for surgery, n	
Anastomosis reconstruction	3
Colectomy	35
Other	1

Supplementary Table 2. Quantitative Polymerase Chain Reaction Primer Sequences

Gene	Direction	Primer sequence
GAPDH	fwd	CGGAGTCAACGGATTGG
GAPDH	rev	TGATGACAAGCTTCCCGTTC
IFN-gamma	fwd	ACTGACTTGAATGTCCAACGCA
IFN-gamma	rev	ATCTGACTCCTTTTTCGCTTCC
TNF	fwd	CTCTTCTGCCTGCTGCTGCACTTTG
TNF	rev	ATGGGCTACAGGCTTGCACTC

Supplementary Table 3. Expansion Medium for Intestinal Organoid Culture

Variable	Final concentration	Company	Catalog no.
AD+++	17.5% (v/v)		
B27 supplement	1×	Thermo Fisher	17504001
N2 supplement	1×	Thermo Fisher	17502001
Murine EGF	50 ng/mL	Peppo-Tech	315-09-500
N-acetyl-L-cysteine	1.25 mM	Sigma-Aldrich	A9165-25G
[Leu15]-gastrin	10 nM	Sigma-Aldrich	G9145-.1MG
Nicotinamide	10 mM	Sigma-Aldrich	N0636-100G
SB202190	10 μ M	Sigma-Aldrich	S7067-25MG
A83-01	500 nM	Tocris	2939/10
Noggin-CM	10% (v/v)	Homemade	—
R-spondin-1-CM	20% (v/v)	Homemade	—
WNT3a-CM	50% (v/v)	Homemade	—